SD-TR-85-61

(12)

20000801198

# Rain Impact Assessment of Advanced Thermal Protection System Materials Phase I Test Results

R. M. COOPER
Materials Sciences Laboratory
Laboratory Operations
The Aerospace Corporation
El Segundo, CA 90245

5 September 1985







Prepared for

SPACE DIVISION
AIR FORCE SYSTEMS COMMAND
Los Angeles Air Force Station
P.O. Box 92960, Worldway Postal Center
Los Angeles, CA 90009-2960

This report was submitted by The Aerospace Corporation, El Segundo, CA 90245, under Contract No. F04701-83-C-0084 with the Space Division, P.O. Box 92960, Worldway Postal Center, Los Angeles, CA 90009-2960. It was reviewed and approved for The Aerospace Corporation by R. W. Fillers, Director, Materials Sciences Laboratory.

Capt Mark D. Borchardt, SD/YNSA, was the project officer for the Mission-Oriented Investigation and Experimentation (MOIE) Program.

This report has been reviewed by the Public Affairs Office (PAS) and is releasable to the National Technical Information Service (NTIS). At NTIS, it will be available to the general public, including foreign nationals.

This technical report has been reviewed and is approved for publication. Publication of this report does not constitute Air Force approval of the report's findings or conclusions. It is published only for the exchange and stimulation of ideas.

Mark D. Borchardt

MARK D. BORCHARDT, Capt, USAF
MOIE Project Officer
SD/YNSA

JOSEPH HESS, GM-15
Director, AFSTC West Coast Office
AFSTC/WCO OL-AB

UNCLASSIFIED

SECURITY CLASSIFICATION OF THIS PAGE (When Data Entered)

| REPORT DOCUMENTATION PAGE | READ INSTRUCTIONS BEFORE COMPLETING FORM |
|---|---|
| 1. REPORT NUMBER: SD-TR-85-61 | 2. GOVT ACCESSION NO.: AD-A162 131 |
| | 3. RECIPIENT'S CATALOG NUMBER |
| 4. TITLE (and Subtitle): RAIN IMPACT ASSESSMENT OF ADVANCED THERMAL PROTECTION SYSTEM MATERIALS: PHASE I TEST RESULTS | 5. TYPE OF REPORT & PERIOD COVERED |
| | 6. PERFORMING ORG. REPORT NUMBER: TR-0084A(5935-04)-2 |
| 7. AUTHOR(s): Robert M. Cooper | 8. CONTRACT OR GRANT NUMBER(s): F04701-83-C-0084 |
| 9. PERFORMING ORGANIZATION NAME AND ADDRESS: The Aerospace Corporation, El Segundo, Calif. 90045 | 10. PROGRAM ELEMENT, PROJECT, TASK AREA & WORK UNIT NUMBERS |
| 11. CONTROLLING OFFICE NAME AND ADDRESS: Space Division, Los Angeles Air Force Station, Los Angeles, Calif. 90009-2960 | 12. REPORT DATE: 5 September 1985 |
| | 13. NUMBER OF PAGES: 67 |
| 14. MONITORING AGENCY NAME & ADDRESS(if different from Controlling Office) | 15. SECURITY CLASS. (of this report): Unclassified |
| | 15a. DECLASSIFICATION/DOWNGRADING SCHEDULE |

16. DISTRIBUTION STATEMENT (of this Report)

Approved for public release; distribution unlimited.

17. DISTRIBUTION STATEMENT (of the abstract entered in Block 20, if different from Report)

18. SUPPLEMENTARY NOTES

19. KEY WORDS (Continue on reverse side if necessary and identify by block number)

Rain erosion
Rain impact
Thermal Protection System (TPS)
Tiles

20. ABSTRACT (Continue on reverse side if necessary and identify by block number)

A rain impact test program, conducted jointly with NASA and AFWAL/UDRI to study the durability of advanced thermal protection system (TPS) materials under exposure to rain conditions typical of flight, has been under way since FY 83. The first test series was conducted in February 1984 at the AFWAL Materials Laboratory Mach 1.2 Rain Erosion Test Facility. Damage threshold levels were bracketed or upper limits established for the

DD FORM 1473 (FACSIMILE)

UNCLASSIFIED

SECURITY CLASSIFICATION OF THIS PAGE (When Data Entered)

19. KEY WORDS (Continued)

20. ABSTRACT (Continued)

rigid TPS materials. The borosilicate glass-coated TPS failed by flexure of the coating, and a rough correlation of rain impact resistance with the compressive modulus of the tile substrate material was found. The durability of the bare tile material was not substantially increased by the use of a SiC coating infiltrated and sintered in the surface layer. The testing technique used with the flexible cloth class of TPS entailed difficulties which precluded the acquisition of valid test data, and alternative approaches for obtaining the desired data are being explored.

## PREFACE

The data presented here are the result of a joint NASA/AFWAL-University of Dayton Research Institute/Aerospace Corporation effort to investigate the rain impact resistance of advanced thermal protection system (TPS) designs.

Chief contributors are:

NASA Ames Research Center

H. Goldstein

D. Leiser

P. Sawko

University of Dayton Research Institute (UDRI)

C. J. Hurley

Thanks are also due to Timothy Courney, University of Dayton Research Institute, for performing the tests in the AFWAL Materials Laboratory Rain Erosion Test Facility; to Noal Tracy, of the Universal Technology Corp., for NDT of test articles; and to John Zeigenhagen, University of Dayton Research Institute, for pre and post test photography of the test articles. Mention must also be made of helpful discussions and tile property data from Mr. Dave Mustelier, Rockwell International, and tile property data from Mr. Ronald Banas, Lockheed Missiles and Space Co. Sound speed measurements on FRCI-20-12 and LI-900 tile samples were carried out by Mr. John R. Linn, of The Aerospace Corporation, Materials Sciences Laboratory.

CONTENTS

FIGURES

FIGURES (Continued)

## TABLES

# I. INTRODUCTION

Rain and ice impact damage has been a continuing concern in the development of atmospheric entry vehicles. Materials that provide thermal protection at hypersonic speeds are not necessarily resistant to rain and ice impact at supersonic and subsonic speeds. In addition, the relationship among material properties, environmental parameters, and flight performance has not been adequately established. For future manned and unmanned lifting entry vehicles, the rain and ice erosion performance of candidate heat shield materials must be evaluated and the mechanism of the erosion process studied. This program addresses the issue of heat shield material performance and is thus intended to contribute to the understanding of the basic physical processes involved.

The development of advanced, reusable military spaceflight systems, advanced space transportation vehicles, and advanced hypersonic cruise vehicles includes the consideration of three options for space vehicle construction: (1) cold or warm structures with operating temperatures of the structural materials limited to less than 700°F by an external thermal protection system; (2) metallic hot structures, operating at structural temperatures on the order of 2000°F with no external thermal protection system (TPS); and (3) carbon-carbon hot aeroshell structures, operating at temperatures on the order of 3500°F.

The current space shuttle system was designed for launch in fair weather only. Initial flight experience has shown that rain and hail impact damage to the orbiter external insulation heat shield on the launch pad and during ferry flight are significant operational concerns for the reusable surface insulation (RSI) system. An RSI that has greater rain resistance for use on the current orbiters and future advanced space transportation systems will result in much more durable and cost-effective vehicles. Therefore, new rigid and flexible ceramic heat shield materials being developed by NASA have improved rain resistance among their development goals.

Advanced military spaceflight and other hypersonic cruise vehicle system requirements include all-weather operation, particularly with regard to launch-on-demand, airborne loiter, and land-on-demand. Accordingly, there is a need to evaluate the rain and hail impact erosion and characteristics of the candidate surface materials to be employed in the various design options, so that realistic and valid specifications and limitations can be applied to each concept. Of concern are advanced TPS materials, hot structure surface coatings, and advanced carbon-carbon materials.

## II. BACKGROUND

At present, there are few applicable rain/hail impact erosion data points for the evaluation of the current space shuttle orbiter TPS or for the assessment of advanced TPS in applications such as the Advanced Military Spaceflight Concept (AMSC), Transatmospheric Vehicle (TAV), and advanced space transportation systems studies. The shuttle orbiter is placarded against launch or ferry flight in rain. The current TPS is not designed to withstand hail or to survive particle impact kinetic energy levels greater than 0.006 foot-pounds normal to the surface.

Limited rain erosion data were obtained[1] during the characterization of silica and mullite tile candidate materials in the early 1970's. The experiments were performed by means of the AFML-Bell Aerospace Company rotating arm rain erosion test apparatus, under the direction of the Air Force Materials Laboratory and with the sponsorship of the NASA Manned Spacecraft Center (now the Lyndon B. Johnson Space Center). All test materials were provided by NASA, and included the Lockheed LI-1500 silica fiber insulation material coated with a silicon carbide pigmented borosilicate glass (LMSC-0042) outer mold line (OML) coating. The tile successfully sustained rain conditions of 1/2-in. per hour for one hour at 350 mph at an angle of incidence of 10 deg; minor surface erosion occurred under the same rain conditions at an angle of incidence of 20 deg for 5 min, and the tile was significantly eroded within 30 sec for a 40 deg angle of incidence, 1/4-in. per hour rain field at 350 mph. The threshold velocity for damage at low angles of incidence in a 1/4-in. per hour rain field was between 300 and 410 mph.

Additional insight into rain impact effects was obtained on HRSI-type tiles with the LMSC-0050 borosilicate glass OML ceramic coating during the Kennedy Space Center RSI Flight Environmental Test Program, conducted between 7 March 1975 and 9 August 1976.[2] The test panel was mounted on the lower fuselage of a twin-engine Beechcraft airplane ("NASA Six") to expose the RSI to the weather and sand-salt atmosphere encountered at KSC. The side wall and a portion of the OML coating were damaged on out-of-specification (0.15-in. as

opposed to the 0.015-in. specification value) forward facing steps presented by the lead tiles in the arrays while on a flight through light-to-moderate showers at an average air speed of 144 mph (125 knots) and a maximum speed of 184 mph (160 knots) during a 2.1 hour flight. Flight altitude was on the order of 10 kfeet.

Experience with shuttle orbiter flights has demonstrated that even severe hail impact damage can be sustained over certain portions of the vehicle TPS where entry heating loads are not high, e.g., fuselage sidewalls, without significant overheating of the underlying substructure. Likewise, localized but severe launch debris impact damage to portions of the lower surface tiles where heat loads are fairly high, such as on the nose landing gear door and on the body flap, and the complete loss of the outer mold line (OML) ceramic coating plus a portion of underlying tile material of six high temperature reusable surface insulation (HRSI) tiles along the right hand chine due to on-orbit ice cracking, did not result in significant substructure overtemperatures during entry even though incipient failure of the RSI did occur. However, where portions of the OMS pod forward section TPS have been lost due to pre-launch hail damage or during launch and ascent, entry heating resulted in graphite-epoxy honeycomb sandwich panel substructure damage of varying degrees of severity. In the most severe case, that due to launch debris impact damage to the lefthand pod during STS-9, it was found necessary to replace a panel of the forward section substructure. Whereas this OMS pod damage has not resulted in shuttle orbiter safety of flight issues because of the localized character of the damage and the absence of critical components behind the damage site, entry heat loads in regions of higher heating could become a safety-of-flight issue in the presence of such TPS damage and loss. The complete loss of the OML coating from two or more adjacent lower surface tiles in critical areas such as aft of the nose cap, at the wing tips and outboard elevon, and on the body flap would be considered very serious, with probable safety-of-flight implications for any entry trajectory. For military operations, the need for TPS and possible substructure replacement would have very undesirable, if not unacceptable, impact on turnaround time between missions.

Concern regarding ice impact on the TPS arose following the first of the orbital flight test launches because of the damage sustained from launch debris impact, including ice from the cryogenic external tank (ET). Considerable progress has been made in eliminating debris sources, in large measure because of a concerted effort by the debris damage team. This activity has been paralleled by an on-going ice impact test program[3] which is evaluating the damage resistance of a broad range of TPS materials. The preliminary phase and Phases 1 through 3 of the program have been completed, providing data on the relative performance of lower surface HRSI/LI-900, LI-2200, reinforced carbon-carbon (RCC), fibrous refractory composite insulation (FRCI), and advanced flexible reusable surface insulation (AFRSI) materials, as well as a class of "enhanced" coatings.

The program results demonstrated the importance of projectile breakup as an energy dissipation mechanism, and, in particular, showed that steel ball drop test data are not a valid basis for estimating ice impact response (because of the lack of the projectile breakup mechanism). The hard ice projectiles used in the test program are considered a good simulation for the hard ice found on some areas of the ET ogive; frozen clear water droplets (icelets) have also been observed on the ET ogive. However, acreage sheet ice found on the ET ogive tends to be "softer" ice which has better breakup characteristics than the hard ice.

The Phase 2 test results indicate that the flexible blanket material experiences gouging to about the same extent as the LI-900 tile damage under similar ice impact conditions. The extrapolation of this ice impact response data to rain impact response prediction is uncertain for several reasons, including the question of how to properly account for the influence of projectile (raindrop) breakup, as well as possible difference in angle of incidence between the ET ice impact scenario and the launch-through-rain scenario.

Very recently, limited single drop and multiple-drop rain impact testing of current TPS materials has been performed by investigators at Rockwell International (RI). Of particular interest is the performance of the HRSI (LI-900), AFRSI, and LRSI materials under conditions simulating a launch

through fog and drizzle. Additional testing was carried out during FY 84 under an internal R and D program.

To initiate the development of a suitable data base summarizing the expected performance of advanced TPS materials of interest to the AMSC and future STS programs under rain impact conditions, including conditions relating to ferry flight or loitering, an informal joint test program with AFWAL/UDRI, NASA Ames Research Center, and AFSTC/Aerospace is in progress. The cooperative effort draws upon the extensive background, experience, and experimental capabilities in the impact erosion technology area that have been developed within the Air Force Wright Aeronautical Laboratories by the Materials Laboratory and UDRI Aerospace Vehicle Coatings Group (C. Hurley). Advanced TPS materials that are being studied by NASA Ames (H. Goldstein) provide the major portion of the rain erosion test matrix. Laboratory examination of the post-test condition of the test articles will be performed jointly by AFWAL/UDRI and The Aerospace Corporation as part of the Laboratory Operations MOIE program.

# III. APPROACH

The broad objectives of the test program are to establish rain impact damage threshold conditions for advanced TPS materials and to collect data for future use in developing empirical and analytical damage prediction models. An attempt will also be made to relate the rain impact damage to the expected reduction in thermal protection provided by the damaged TPS to typical lifting entry vehicle substructures.

Two classes of TPS materials were evaluated in Phase I of the program: (1) flexible ceramic insulation blanket materials, and (2) rigid reusable surface insulation (RSI) materials. The rigid RSI materials were examined both with and without the reaction cured glass (RCG) ceramic coatings needed to provide the surface optical properties necessary for space vehicle orbital and entry functions as well as to provide moisture protection for the tile. One set of samples included a developmental tile coating formed by chemical vapor deposition of SiC in the tile surface. The response of carbon-carbon composite material such as currently used for nose cap and wing leading edge and proposed for aeroshell construction of future STS configurations will be studied later in the test program. The performance of multi-wall metallic TPS designs also is of interest and an effort will be made to acquire and test prototype test articles later in the program.

## IV. TEST PROGRAM

### A. FACILITIES

The rain erosion experimentation is being carried out in the AFWAL Mach 1.2 Rain Erosion Test Facility (described in Ref. 4) using a calibrated 1-in. per hour simulated rainfall of 2.0 mm dia. (avg.) drops. During the Phase I tests, the 90 deg impact angle specimen-configuration 2 (Figure 1) was used, with the standard titanium cover plate (Figure 2) having a 1.87 by 0.8 inch exposure area, held in the standard stainless steel sample holder (Figure 3), which is bolted to the test facility whirling arm. One test series was also carried out using the 45 deg impact angle specimen geometry (configuration 6), shown in Figure 4.

### B. TPS MATERIAL DESCRIPTION

The Phase I test matrix included two general classes of TPS: advanced flexible ceramic blanket insulation and rigid ceramic fiber insulation materials. Other classes, such as carbon-carbon (RCC/ACC) and metallic TPS will be added as they become available.

#### 1. Advanced Flexible Ceramic Blanket Insulation

The flexible blanket configuration parameters are:

a. Outer Mold Line (OML) fabric material, thickness, and sizing

b. Internal insulation material, thickness and density

c. OML thread material, thickness, sizing, and stitching patterns

The baseline flexible blanket material is the AFRSI initially used on the OMS pods of shuttle orbiter OV-099 and on the upper surfaces of OV-103. The blanket typically consists of the Type 2, heavy, 0.027-in. Astroquartz 570 silica OML cloth layer stitched over a nominal 0.045-in. thick (Class 1) microquartz Q-felt internal insulation material with 0.020-in. dia. Teflon-sized silica thread. The blankets are waterproofed with Dow Corning Z 6070 Silane, the same waterproofing agent used in the rigid TPS on shuttle orbiter vehicles.

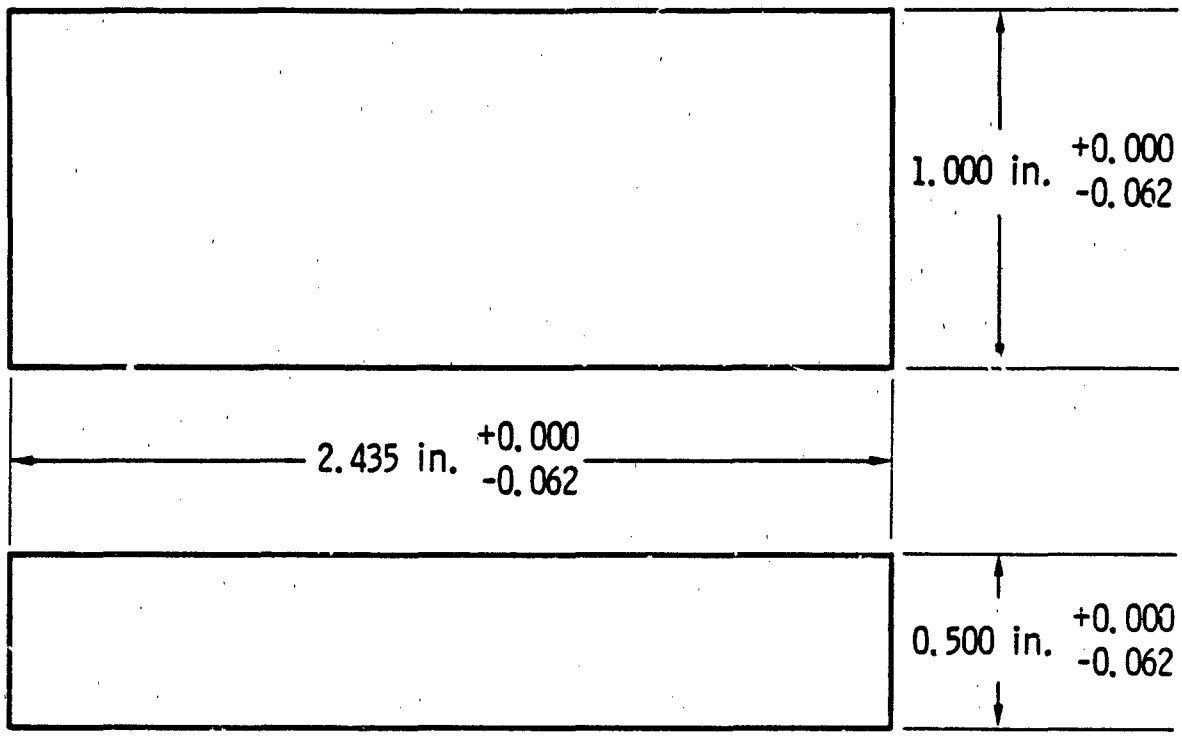


ALL DIMENSIONS IN INCHES

Fig. 1. 90° Impact Angle Specimen - Configuration 2

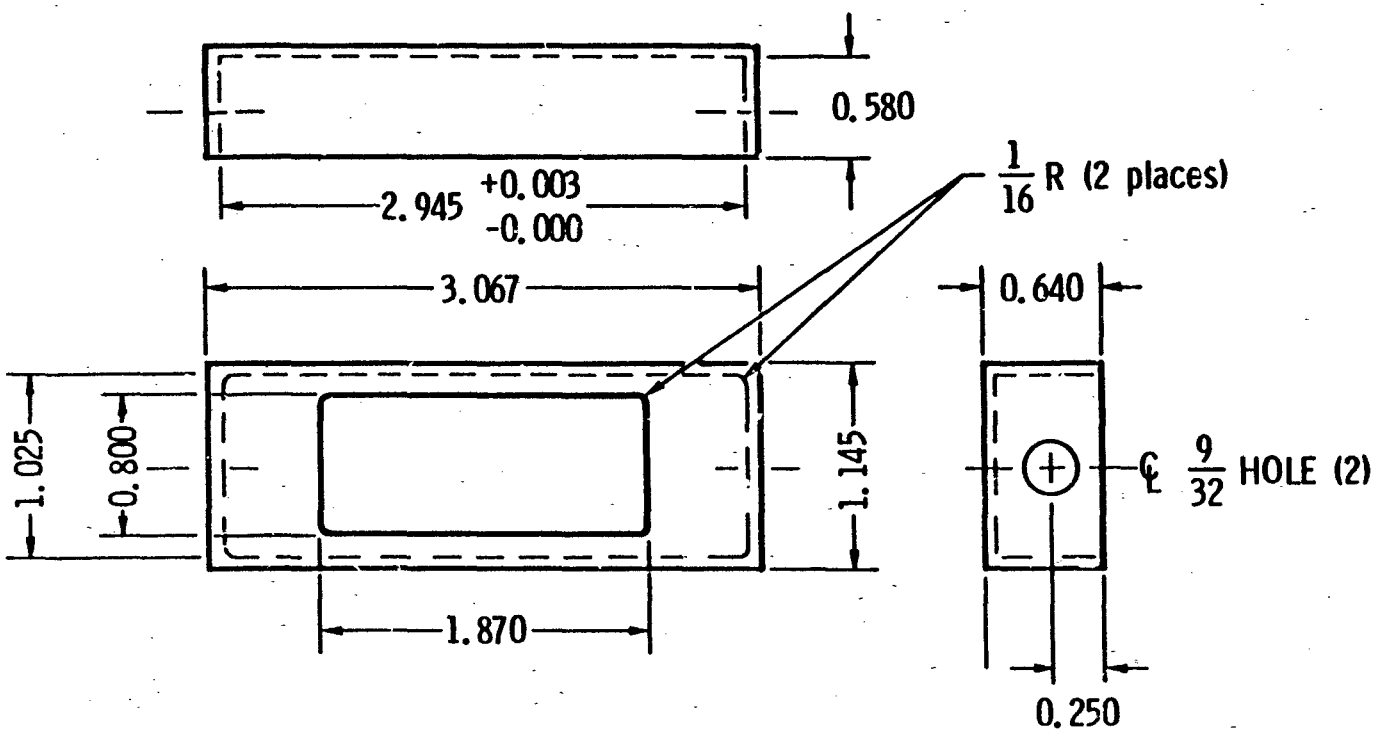


Fig. 2. 90° Sample Cover Plate

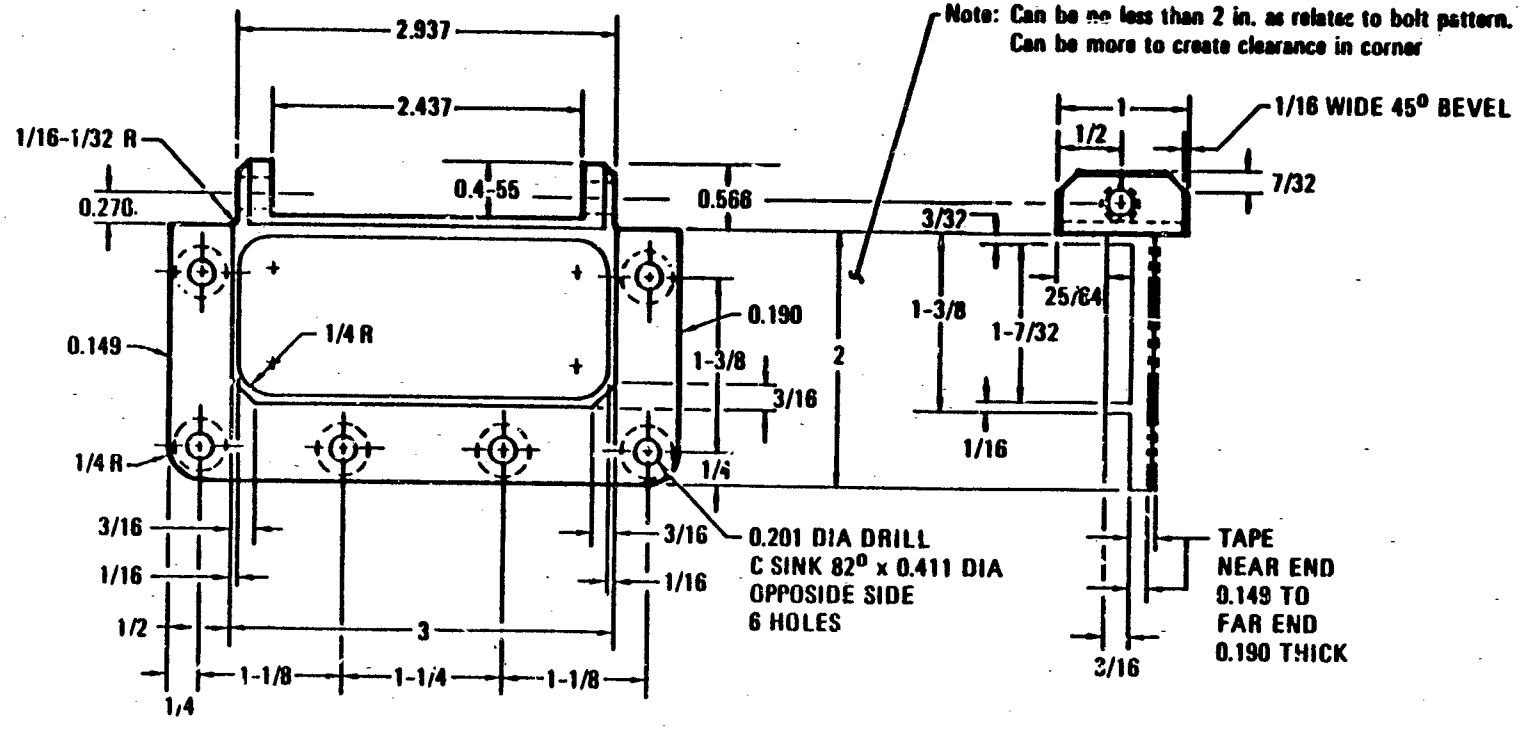


Fig. 3. Sample Holder

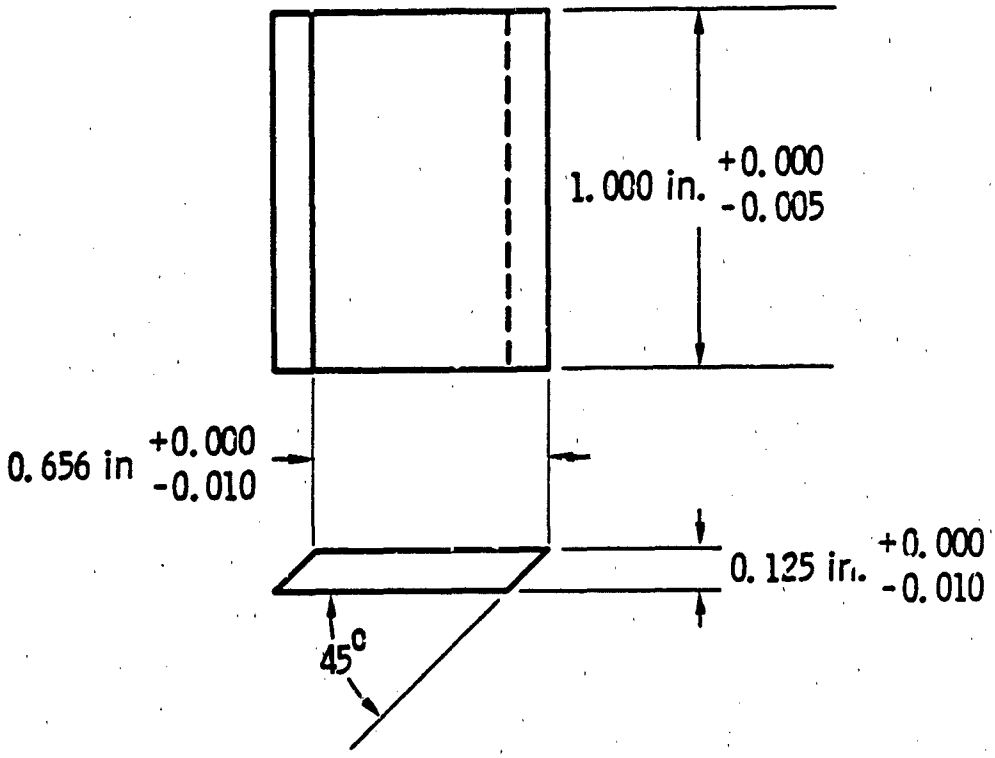


Fig. 4. 45° Impact Angle Specimen - Configuration 6

In Phase I of this program, only the OML cloth materials were tested. Because size effects are critical in the performance of flexible ceramic insulation blankets, sample holder size limitations make it doubtful that a valid simulation of a complete blanket is possible and results could be misleading. It was hoped that testing one element of the flexible ceramic insulation blanket, such as the OML cloth layer would permit the candidate materials to be compared. A common backing material, the felt RSI (FRSI) material, was used as the substrate material backing the candidate test cloth materials.

The baseline AFRSI cloth material was heat cleaned and waterproofed and was tested as is (i.e., with no additional coating); with a Rockwell ceramic coating identified as the C-9 coating; and with a NASA Ames RC ceramic coating (ACC). The Rockwell C-9 coating is a high purity formulation of deionized Ludox (MB0115-011) and ground silica (MB0115-036) applied after a primer or pre-coat of deionized Ludox and isopropyl alcohol has been used to deactivate the waterproofing and provide a base coat for improved adhesion to the OML cloth layer.

The experimental OML cloth fabric materials to be studied were Nextel-312 (900 denier) fabric, manufactured from aluminoborosilicate fibers by 3M Corporation, and Nicalon, manufactured by Nippon Carbon, a silicon carbide fabric that recently became available. The Nextel-312 and Nicalon OML cloth layers were heat cleaned and waterproofed. The flexible ceramic blanket materials are described in Table 1.

2. Rigid Ceramic Fiber Insulation

The rigid ceramic fiber insulation material configuration parameters are: (1) tile substrate materials and thickness, (2) OML ceramic coating materials and thickness, and (3) waterproofing (Dow Corning Z-6070 Silane). The baseline rigid ceramic fiber insulation material in this program is FRCI-20-20, a second generation tile material that has shown considerable resistance to crack propagation. At the present time, FRCI-20-12 has been flight qualified and is being used on shuttle orbiter vehicle-103. The FRCI material is a composite of two ceramic fibers plus a small percentage of silicon carbide, which is added as an opacifier and emittance agent to provide

lower thermal conductivity and improved optical properties. In the FRCI material designation, the first number is the percent of aluminoborosilicate fiber, and the remainder is the same silica fiber (microquartz) that is used in the first generation RSI. The second number is the tile density in pounds per cubic foot. For comparison, current shuttle orbiter tile materials, fabricated from the pure silica fiber (microquartz) only, were tested. The material designations are LI-900 (9 pounds per cubic foot density) and LI-2200 (22 pounds per cubic foot density). The FRCI-20-20, FRCI-20-12, LI-2200, and LI-900 tile materials were exposed to rain impact with and without the baseline doped borosilicate reaction cured glass (RCG) OML ceramic coating. In addition, chemical vapor deposited (CVD) silicon carbide (SiC) coatings of 2.5 weight percent and 5.0 weight percent were applied to LI-2200, FRCI-40-20, FRCI-60-20, and alumina-enhanced thermal barrier (AETB) material, AETB-40-20, test samples. AETB material is an experimental advanced rigid tile material being developed by NASA Ames Research Center. With two exceptions, all test samples were waterproofed following current fabrication procedures.

Table 1. Advanced Flexible Ceramic Blanket TPS Materials Description

| Source | OML Cloth Material | OML Cloth Thickness, mil | Coating Material |
|---|---|---|---|
| Rockwell Production Line | Type 2, heavy Astroquartz 570 | 27 | None<br>RCC<br>ACC |
| | Type 1, light Astroquartz 593 | 10 | None<br>RCC<br>ACC |
| 3M/Ames Research Material | Nextel-312, heavy (900 denier) | | None<br>ACC |
| Dow Corning/Ames Research Material | Nicalin SiC | | None<br>ACC |

RCC - Rockwell Ceramic Coating (C-9) High Purity ludox and silica.

ACC - Ames Research Center Ceramic Coating.

One standard thickness (0.015 in.) was used on all RCG coated test samples with the exception of the FRCI-20-12 material, which also included samples with twice the standard RCG coating thickness. Sets of test articles with a minimum of six test samples are designated "nominal" sets. In addition, four of the more readily available tile material configurations were used in preliminary scoping test runs to calibrate the test rain field and establish the order of magnitude of the velocities just producing damage in the four different tile substrate materials. These sets contained more than the minimum number of six samples, and are designated as "calibration" sets. The rigid tile materials are described in Table 2.

## C. PHASE I TEST MATRIX

The prioritized test matrix for the Phase I experiments is given in Table 3. The first priority for the rigid tile materials was the baseline FRCI-20-20, which was expected to show the best performance, based upon current knowledge of materials behavior. If this material did not survive at the lowest calibrated test speed of the facility, there was no point in testing the other coated rigid tile materials listed in the first group, because they were believed to be weaker than the baseline material. The four cloth materials and the unwaterproofed water-filled FRCI-20-20 samples followed as shown. Testing of the uncoated rigid tile samples depended upon the performance of the coated materials. The lowest speed of interest in seeking the damage threshold level for any material has been selected to be 100 mph, although a higher lower limit (e.g., 120 or 130 mph) would have been acceptable. The rationale for the initial test speed selection is given in the following paragraphs.

### 1. Advanced Flexible Ceramic Blanket Insulation

Neither empirical extrapolation of existing data nor analytical modelling approaches were available for predicting the damage threshold levels for these materials. Accordingly, estimates of the likely damage threshold velocities for the advanced flexible ceramic blanket insulation materials had large uncertainties because of the lack of knowledge or data on rain impact effects on such materials. The results of Phase 2 of the Ice Impact Testing Program

## Table 2. Rigid Ceramic Fiber Insulation

| Source | Tile Substrate Material | Tile Coating Material | Coating Thickness | Set | Six test articles per nominal set Calibration Set contains more than six test articles (total number TBD) |
|---|---|---|---|---|---|
| LMSC Production Line | LI-900 | -- | -- | Calibration | |
| | LI-900 | RCG | 15 mil | Calibration | Rigid Low Density Ceramic Tiles |
| | LI-900 | RCG | 30 mil | Nominal | |
| | LI-900 | RCG | 45 mil | Nominal | LI-series: Rigidized high-silica microquartz fibers |
| | LI-2200 | - | - | Calibration | |
| | LI-2200 | RCG | 15 mil | Calibration | FRCI-series: Rigidized composite of high-silica microquartz fibers and alumino borosilicate fibers plus 2% SiC powder |
| | LI-2200 | RCG | 30 mil | Nominal | |
| | LI-2200 | CVD SiC | 2.5 wt % | Nominal | |
| | LI-2200 | CVD SiC | 5 wt % 0.0234 lb/ft$^2$ | Nominal | |
| | FRCI-20-12 | - | - | Calibration | |
| | FRCI-20-12 | RCG | 15 mil | Nominal | |
| | FRCI-20-12 | RCG | 30 mil | Nominal | Ceramic coatings |
| | FRCI-20-12 | RCG | 45 mil | Nominal | |
| LMSC Pilot Plant | FRCI-20-20 | - | - | Nominal W,UFW | RCG-reaction cured borosilicate glass with silicon tetraboride additive |
| | FRCI-20-20 | RCG | 15 mil | Nominal W,UFW,W(45°) | |
| Babcock & Wilcox | FRCI-40-20 | - | - | Calibration | CVD SiC - chemical vapor deposited silicon carbide |
| | FRCI-40-20 | RCG | 15 mil | Nominal | |
| | FRCI-40-20 | CVD SiC | 2.5 wt % | Nominal | Applied to tiles by Americom, Inc. |
| | FRCI-40-20 | CVD SiC | 5 wt % 0.0456 lb/ft$^2$ | Nominal | |
| Ames Research Tile | FRCI-60-20 | - | - | Nominal | |
| | FRCI-60-20 | RCG | 15 mil | Nominal | |
| | FRCI-60-20 | CVD SiC | 2.5 wt % 0.0738 lb/ft$^2$ | Nominal | |
| | AETB-40-20 | CVD SiC | 0.049 lb.ft$^2$ | Nominal | |

## Table 3. Phase I Test Matrix (Angle of Incidence Normal to Surface)

| Priority | Material | Condition | Coating | Coating Thickness | Initial Test Speed, MPH | Duration sec. | Comments |
|---|---|---|---|---|---|---|---|
| 1 | FRCI-20-20 | W | RCG | ST | 380 | 60 | Reduce speed until sample survives |
| 1a | LI-2200 | W | RCG | ST | See Comments | 60 | Start with survival speed of FRCI-20-20[a] |
| 1b | FRCI-20-12 | W | RCG | ST[b] | See Comments | 60 | Start with survival speed of LI-2200[c] |
| 1c | LI-900 | W | RCG | ST | See Comments | 60 | Start with survival speed of FRCI-20-12[d] |
| 1d | FRCI-20-20 | UFW | RCG | ST | See Comments | 60 | Start with survival speed of FRCI-20-20 |
| 1e | FRCI-20-20[e] | W | RCG | ST | --- | 60 | 45-deg angle of incidence (configuration 5) |
| 2 | "Baseline" AFRSI Cloth | HC & WR | None | --- | 300 | 60 | Reduce speed until sample survives |
| 2a | "Baseline" AFRSI Cloth | HC & WR | RCC | --- | 300 | 60 | Reduce speed until sample survives |
| 2b | "Baseline" AFRSI Cloth | HC & WR | ACC | --- | 300 | 60 | Reduce speed until sample survives |
| 2c | "Baseline" AFRSI Cloth[e] | HC & WR | None | --- | --- | 60 | 45-deg angle of incidence (configuration 5) |
| 3 | Nextel AFRSI Heavy Cloth | HC & WA | None | --- | 300 | 60 | Reduce speed until sample survives |
| 3a | Nextel AFRSI Heavy Cloth | HC & WA | ACC | --- | 300 | 60 | Reduce speed until sample survives |
| 4 | Nicalon AFRSI Cloth | HC & WA | None | --- | 300 | 60 | Reduce speed until sample survives |
| 4a | Nicalon AFRSI Cloth | HC & WA | ACC | --- | 300 | 60 | Reduce speed until sample survives |
| 5 | FRCI-20-20 | W | None | --- | See Comments | 60 | Start with survival speed of coated FRCI-20-20 (1) |
| 5a | FRCI-20-20 | UFW | None | --- | See Comments | 60 | Start with survival speed of coated FRCI-20-20 (1) |
| 6 | LI-2200 | U | None | --- | See Comments | 60 | Start with survival speed of coated LI-2200 (1a) |
| 6a | LI-2200 | W | $SiC_{CVD}$ | (2.5%) | See Comments | 60 | Start with survival speed of coated LI-2200 (1a) |
| 6b | LI-2200 | W | $SiC_{CVD}$ | 0.0234 lb/ft$^2$ | See Comments | 60 | Start with survival speed of coated LI-2200 (1a) |
| 7 | FRCI-40-20 | W | None | --- | 380 | 60 | Reduce speed until sample survives |
| 7a | FRCI-40-20 | W | $SiC_{CVD}$ | (2.5%) | 380 | 60 | Reduce speed until sample survives |
| 7b | FRCI-40-20 | W | $SiC_{CVD}$ | 0.0456 lb/ft$^2$ | 380 | 60 | Reduce speed until sample survives |
| 8 | FRCI-20-12 | W | RCG | 2 x ST[b] | See Comments | 60 | Start with survival speed of coated FRCI-20-12 (1b) |
| 9 | FRCI-60-20 | W | $SiC_{CVD}$ | 0.0738 lb/ft$^2$ | 380 | 60 | Reduce speed until sample survives |
| 10 | AETB-40-20 | W | $SiC_{CVD}$ | 0.049 lb/ft$^2$ | 380 | 60 | Reduce speed until sample survives |

W - Waterproofed
UFW - Unwaterproofed full of water
HC & WR - Heat cleaned and waterproofed at Rockwel
HC & WA - Heat cleaned and waterproofed at Rockwe..
RCC - Rockwell ceramic coating
ACC - Ames ceramic coating
RCG - Reaction cured glass coating (standard)
U - Unwaterproofed
ST - Standard thickness (15 mil)
$SiC_{CVD}$ - Silicon carbide - chemical vapor deposited
(45°) 45° impact angle specimens

a - Discontinue 1a, b, c, if survival speed of FRCI-20-20 is too low (~ 100 mph)
b - Coating thicknesses actually reversed; 1b has 2x std and 8 has std thickness.
c - Discontinue 1b, c if survival speed of LI-2200 is too low.
d - Discontinue 1c if survival speed of FRCI-20-20 is too low.
e - Samples 1e and 2c to be run at 45-deg angle of incidence (configuration 5) when expedient.

(Ref. 3) indicated that the AFRSI blanket material damage was similar to that for the LI-900 tiles tested during Phase 1. Since all materials tested were significantly damaged under the prescribed test conditions, damage threshold levels were not available.

Recent RI results indicate that AFRSI performance was superior to that of LRSI, which uses the LI-900 tile material with a 10 mil white 0036 ceramic OML coating, when exposed to drizzle-type conditions (average drop size 0.7 mm dia.). No data were available for the Nextel-312 or Nicalon SiC cloth materials. On the basis of available data, an initial test speed of 300 mph was selected.

2. Rigid Ceramic Fiber Insulation

The data from RI provided some insight into the probable damage mechanism and a basis for extrapolation to the normal incidence, 2.0 mm dia. drop size case of interest here. Local flexural failure of the RCG OML ceramic coating in the vicinity of a water drop impact at a speed of 200 mph appeared to be a reasonable expectation for the coated FRCI-20-20 material. This speed is somewhat higher than the zeroth order extrapolation to 120 mph which can be made from the 1972 data (Ref. 1) mentioned in Section II, where a less dense (LI-1500, 15 pounds per cubic foot density) tile material with a type-0042 borosilicate glass coating of unreported thickness was used. The 120 mph is the velocity component normal to the surface from the 20 deg angle of incidence, 1-in. per hour rainfall data in Ref. 1, where only slight erosion of the coated LI-1500 test article was found. The actual damage threshold velocity for normal impact was expected to be somewhat less than 120 mph, on the basis of observations given in the literature (see Ref. 5 for an extensive list of references). For example, less damage occurred in infrared transmitting materials under shallower angles of impact than in the normal impact case with the same normal component of velocity.[6] Likewise, the KSC flight through light-to-moderate rain resulted in substantial side wall damage with an average flight speed of 144 mph (125 knots) and a maximum speed of 184 mph (160 knots), i.e., on the same order as indicated by the Ref. 1 data.

The higher density, stronger FRCI-20-20 was expected to have a higher damage threshold level. Experience at UDRI obtained over a number of years with the rain erosion test apparatus indicates that the flight test situation in which the forward facing step was present at the damage site resulted in a more severe condition than would be produced under the 90 deg normal impact test configuration; this suggests a higher damage threshold here. This is because of trapping or channelling of water and energy into a "corner", with no other place to go, in the KSC flight situation.

Raindrop deformation and travel after impact transfers three or four times as much energy as is imparted on initial impact. The variation of damage with angle of incidence is therefore more complicated than a simple dependence on the normal component of the drop velocity. The empirical extrapolation of experimental data as well as the interpretation of the flight test data must be understood to contain some level of risk.

## D. TEST PHILOSOPHY

A number of performance characteristics must be established to determine the relative ranking of candidate advanced TPS materials under rain impact conditions. These characteristics include single mission failure levels, single mission replacement levels, and reduction in mission lifetime. Single mission failure levels are those conditions of velocity and rain rate for which TPS rain impact damage results in significant or catastrophic vehicle substructure damage caused by entry heating effects. Single mission replacement levels are those conditions under which TPS rain impact damage during launch will require TPS replacement before the next flight. This performance characteristic could be critical to mission control decisions regarding launch under adverse weather conditions and could define the space system launch-on-demand capability. Reduced TPS mission lifetime caused by rain impact during launch also affects overall launch-on-demand, airborne loiter, and land-on-demand capability.

While determination of the single mission failure and replacement levels appears to be reasonably straightforward, reduction in TPS mission lifetime may be more difficult to interpret, because the effects of entry heat cycling

and rewaterproofing operations between flights, in some cases, may result in synergistic effects on rain impact response and damage accumulation.

It is beyond the scope of this preliminary program to address all these performance issues for the selected test materials. The test philosophy adopted here is to develop as much data as possible regarding damage mechanisms, levels of performance, and material response to support further analytical and experimental studies of TPS resistance to rain impact.

The 90 deg impact angle specimen, configuration 2 (see Figure 1), of the AFWAL Mach 1.2 Rain Erosion Test Facility was selected for Phase I testing, for several reasons. The configuration 2 test sample holder permits specimens with thicknesses close to those of operational interest, and the impact angle is relatively close to conditions which could be encountered on the shuttle orbiter vehicle OMS pods, which probably experience the most severe rain environment. It is also reasonable to assume, on the basis of AFWAL/UDRI experience, that the data can be extrapolated to lower angle of incidence cases without disturbing the relative ranking of the various candidate materials.

The damage threshold level for a given test material is defined as the lowest speed for which damage to the exposed test article is observed with the unaided eye. Thus, damage characterization places emphasis on the integrity and damage mechanisms experienced by the OML layer; the condition of the ceramic coating on the rigid ceramic fiber insulation TPS and of the OML cloth layer on the advanced flexible ceramic blanket insulation TPS is considered to be of primary importance in post-impact TPS performance.

# V. PHASE I TEST RESULTS

## A. SUMMARY

The Phase I testing was successful in bracketing damage threshold levels for three of the KCG-coated test materials (LI-2200, FRCI-20-20, and FRCI-20-12 having twice the standard 15 mil coating thickness). The damage threshold level was less than 150 mph for LI-900 and FRCI-20-12 with standard coating thickness and the bare tile materials (LI-2200, LI-900, FRCI-20-12, FRCI-20-20, and FRCI-40-20). The CVD SiC-coated test articles (LI-2200, FRCI-40-20, FRCI-60-20, and AETB-40-20) failed at or below 150 mph under 30 sec exposure durations. Difficulties with the testing technique precluded valid test data on the flexible cloth layers, because of complications arising from cloth layer mounting constraints and coupling between sample distortion and centrifugal force loads on the test samples. Alternatives to the present approach are needed to provide valid test data on the flexible blanket class of materials.

## B. RIGID TPS TEST RESULTS

Table 4 is a summary of the normal impact test results for the rigid tile class of materials. The procedure followed during the test runs was to monitor the visual condition of the test articles using a closed circuit TV system employing stroboscopic stop motion techniques. The test samples were first brought up to the desired speed on the whirling arm and then the rainfield was turned on, starting the rainfield timing clock. For the bulk of the tests, the test duration was 30 sec. The test run was considered complete when the rainfield was shut off. The time of occurrence of surface damage (made evident by the sudden appearance of a white spot on the black tile coating, or a perceptible blemish on the white surface of uncoated tile samples) was noted to the nearest 0.05 minutes (3 sec) on the rainfield timing clock. The surface damage time reported is believed to be accurate to ± 1 sec, based on past experience with the apparatus. Exceptions to the 30 sec runs were made when extensive damage occurred early in the run, in which event the run was terminated, or when no surface damage was apparent, and a 60 sec run was made.

Table 4. Phase I Test Results Summary (1 in.-hr rainfield, 2.0 mm raindrop, normal impact)

| Priority | Material | AFWAL No. | Comments | Speed MPH | Duration sec | AFWAL/UDRI Category |
|---|---|---|---|---|---|---|
| 1 | FRCI-20-20/ 15 mil RCG coating (waterproofed) | 14939 14940 | 3% of surface area damaged. Isolated minute surface cracks which begin at coating/substrate interface | 200 | 30 | Erosion damage |
| | | 14941 | 15% of surface area damaged, coating penetrated within 3 sec, surface cracks, subsurface fracture, substrate damage | 300 | 3 | Erosion failure |
| | | 14942 | 20% of surface area damaged, coating penetrated within 3 sec, surface cracks, subsurface fractures, substrate damage, average depth of penetration 49 mils | 300 | 3 | Erosion failure |
| | | 14943 | 12% of surface area damaged, coating penetrated within 6 sec, surface cracks, subsurface fractures | 250 | 6 | Erosion failure |
| | | 14944 | 20% of surface area damaged, coating penetrated within 6 sec, surface cracks, subsurface fractures, substrate damage, average depth of penetration 62 mils | 250 | 6 | Erosion failure |

Table 4. Phase I Test Results Summary (1 in.-hr rainfield, 2.0 mm raindrop, normal impact) (Continued)

| Priority | Material | AFWAL No. | Comments | Speed MPH | Duration sec | AFWAL/UDRI Category |
|---|---|---|---|---|---|---|
| 1a | LI-2200/15 mil RCG coating (waterproofed) | 14499 | 75% of surface area damaged, coating penetrated between 12-18 sec, surface cracks, subsurface fractures, substrate damage, average depth of penetration 187.5 mils | 200 | 30 | Erosion failure |
| | | 14500 | 65% of surface area damaged, 1% surface coating penetration between 12-18 sec, surface cracks, subsurface fractures | 200 | 30 | Erosion failure |
| | | 14501 | 65% surface area damaged, coating penetrated between 12-18 sec, surface cracks, subsurface fractures, substrate damage, average depth of penetration 197 mils | 200 | 30 | Erosion failure |
| | | 14502 | 70% surface area damaged, coating penetrated between 12-18 sec, surface cracks, subsurface fractures, substrate damage | 200 | 30 | Erosion failure |
| | | 14503 | 3% surface area damaged, surface cracks, subsurface fracture, no substrate damage | 150 | 60 (30+30) | Erosion damage |
| | | 14504 | No coating or substrate damage | 150 | 60 (30+30) | No damage |

Table 4. Phase I Test Results Summary (1 in.-hr rainfield, 2.0 mm raindrop, normal impact) (Continued)

| Priority | Material | AFWAL No. | Comments | Speed MPH | Duration sec | AFWAL/UDRI Category |
|---|---|---|---|---|---|---|
| 1b | PRCI-20-12 30 mil RCG coating (waterproofed) | 14945 | 15% surface area damaged, surface cracks, subsurface fractures, damage occurred between 60 and 90 sec. | 200 | 90 (30+60) | Erosion damage |
| | | 14946 | 12% surface area damaged, surface cracks, subsurface fractures, damage occurred between 60 and 90 sec | 200 | 90 (30+60) | Erosion damage |
| | | 14947 | 3% surface area damaged, small surface cracks, subsurface fracture, damage occurred between 30 and 60 sec | 200 | 60 (30+30) | Erosion damage |
| | | 14948 | 1% surface area damaged, two small surface cracks, subsurface fractures, damage occurred between 30 and 60 sec | 200 | 60 (30+30) | Erosion damage |
| | | 14949 14950 | No coating or substrate damage | 200 | 30 | No damage |
| | | 14951 | 90% surface area damaged, coating penetration initiated at 12 sec, surface cracks, pitting, substrate damage, average depth of penetration 218 mils | 250 | 30 | Erosion failure |
| | | 14952 | 80% surface area damaged, coating penetration initiated at 12 sec, surface cracks, subsurface fractures, substrate damage | 250 | 30 | Erosion failure |
| | | 14953 14954 | No coating or substrate damage | 150 | 60 (30+30) | No damage |

Table 4. Phase I Test Results Summary (1 in.-hr rainfield, 2.0 mm raindrop, normal impact) (Continued)

| Priority | Material | AFWAL No. | Comments | Speed MPH | Duration sec | AFWAL/UDRI Category |
|---|---|---|---|---|---|---|
| 1c | LI-900/15 mil RCG coating (waterproofed) | 14479<br>14480 | 95% surface area damaged, coating penetrated at 6 sec, substrate damage, complete penetration of substrate | 200 | 30 | Erosion failure |
| | | 14481 | 20% surface area damaged, coating penetrated, surface cracks, substrate damage | 150 | 18 | Erosion failure |
| | | 14482 | 60% surface area damaged, coating removed by 18 sec, surface crack, substrate damage, average depth of penetration 171 mils | 150 | 18 | Erosion failure |
| 1d | FRCI-20-20/15 mil RCT coating (unwaterproofed & full of water) | 14955 | 10% surface area damaged, isolated subsurface fractures | 200 | 30 | Erosion damage |
| | | 14956 | 5% surface area damaged, three isolated subsurface fractures | 200 | 30 | Erosion damage |
| | | 14957 | 90% surface area damaged, coating penetrated at 18 sec, surface cracks, subsurface fractures, substrate damage, average depth of penetration 113 mils | 250 | 30 | Erosion failure |
| | | 14958 | 80% surface area damaged, coating penetrated at 18 sec, surface cracks, substrate damage | 250 | 30 | Erosion failure |
| | | 14959<br>14960 | 3% surface area damaged, surface pitting | 150 | 60 (30+30) | Erosion damage |

Table 4. Phase I Test Results Summary (1 in.-hr rainfield, 2.0 mm raindrop, normal impact) (Continued)

| Priority | Material | AFWAL No. | Comments | Speed MPH | Duration sec | AFWAL/UDRI Category |
|---|---|---|---|---|---|---|
| 5 | FRCI-20-20 Bare (unwaterproofed) | 14521 | 90% surface area damaged, crater formation with some channeling | 200 | 30 | Erosion damage |
| | | 14522 | 85% surface area damaged, crater formation with some channeling, average depth of penetration 72 mils | 200 | 30 | Erosion damage |
| | | 14523 | 20% surface area damaged, crater formation | 150 | 6 | Erosion damage |
| | | 14524 | 30% surface area damaged, crater formation, average depth of penetration 23 mils | 150 | 6 | Erosion damage |
| 5a | FRCI-20-20 bare (unwaterproofed and filled with water) | 14526 | 95% surface area damaged, crater formation with channeling | 200 | 30 | Erosion damage |
| | | 14527 | 95% surface area damaged, crater formation with channeling, average depth of penetration 68 mils | 200 | 30 | Erosion damage |
| | | 14528 | 35% surface area damaged, crater formation, damage initiation within 6 sec | 150 | 12 | Erosion damage |
| | | 14529 | 35% surface area damaged, crater formation, average depth of penetration 18 mils, damage initiation within 6 sec | 150 | 12 | Erosion damage |

Table 4. Phase I Test Results Summary (1 in.-hr rainfield, 2.0 mm raindrop, normal impact) (Continued)

| Priority | Material | AFWAL No. | Comments | Speed MPH | Duration sec | AFWAL/UDRI Category |
|---|---|---|---|---|---|---|
| 6 | LI-2200 (waterproofed) | 14489 | 95% surface area damaged, crater formation and channeling, damage initiation within 3 sec | 200 | 30 | Erosion damage |
| | | 14490 | 95% surface area damaged, crater formation and channeling, average depth of penetration 190 mils, damage initiation within 3 sec | 200 | 30 | Erosion damage |
| | | 14491 | 25% surface area damaged, crater formation, damage initiation within 3 sec | 150 | 3 | Erosion damage |
| | | 14492 | 30% surface area damaged, crater formation, average depth of penetration 68 mils, damage initiation within 3 sec | 150 | 3 | Erosion damage |
| 6b | LI-2200/ .0234#/ft$^2$ SiC (CVD) (waterproofed) | 14913 | 90% surface area damaged, penetration within 3 sec, crater formation and channeling | 200 | 30 | Erosion failure |
| | | 14914 | [illegible]% surface area damaged, penetration within 3 sec, crater formation and channeling, average depth of penetration 245 mils | 200 | 30 | Erosion failure |
| | | 14915 | 25% surface area damaged, coating penetration initiated within 3 sec, crater formation | 150 | 6 | Erosion failure |
| | | 14916 | 30% surface area damaged, coating penetration initiated within 3 sec, crater formation, average depth of penetration 82 mils | 150 | 6 | Erosion failure |

Table 4. Phase I Test Results Summary (1 in.-hr rainfield, 2.0 mm raindrop, normal impact) (Continued)

| Priority | Material | AFWAL No. | Comments | Speed MPH | Duration sec | AFWAL/UDRI Category |
|---|---|---|---|---|---|---|
| 7 | FRCI-40-20 bare (waterproofed) | 14531 | 90% surface area damaged, crater formation with channeling, average depth of penetration 60 mils, damage initiated within 18 sec | 200 | 30 | Erosion damage |
| | | 14532 | 95% surface area damaged, crater formation with channeling, damage initiated within 18 sec | 200 | 30 | Erosion damage |
| | | 14533 | 30% surface area damaged, crater formation, damage initiated within 9 sec | 150 | 12 | Erosion damage |
| | | 14534 | 30% surface area damaged, crater formation, average depth of penetration 18 mils, damage initiated within 9 sec | 150 | 12 | Erosion damage |
| 7a | FRCI-40-20/ 2.5% SiC (CVD) (waterproofed) | 14541 | 40% surface area damaged, coating penetrated within 18 sec, surface pitting, crater formation, substrate damage | 200 | 30 | Erosion failure |
| | | 14542 | 50% surface area damaged, coating penetrated within 18 sec, surface pitting, crater formation, substrate damage, average depth of penetration 80 mils | 200 | 30 | Erosion failure |

Table 4. Phase I Test Results Summary (1 in.-hr rainfield, 2.0 mm raindrop, normal impact) (Continued)

| Priority | Material | AFWAL No. | Comments | Speed MPH | Duration sec | AFWAL/UDRI Category |
|---|---|---|---|---|---|---|
| 7b | FRCI-40-20/ .0456#/Ft$^2$ SiC (CVD) (waterproofed) | 14925 | 35% surface area damaged, surface pitting, crater formation | 200 | 30 | Erosion damage |
| | | 14926 | 35% surface area damaged, surface pitting, crater formation, average depth of penetration 25 mils | 200 | 30 | Erosion damage |
| | | 14927 | 10% surface area damaged, surface pitting, crater formation | 150 | 30 | Erosion damage |
| | | 14928 | 10% surface area damaged, surface pitting, crater formation, average depth of penetration 25 mils | 150 | 30 | Erosion damage |

Table 4. Phase I Test Results Summary (1 in.-hr rainfield, 2.0 mm raindrop, normal impact) (Continued)

| Priority | Material | AFWAL No. | Comments | Speed MPH | Duration sec | AFWAL/UDRI Category |
|---|---|---|---|---|---|---|
| 8 | FRCI-20-12/15 mil RCG coating (waterproofed) | 15016 | 90% surface area damaged, coating penetrated within 12 sec, substrate damage, average depth of penetration 190 mils | 200 | 30 | Erosion failure |
| | | 15017 | 90% surface area damaged, coating penetrated within 12 sec, substrate damage | 200 | 30 | Erosion failure |
| | | 15018 | 90% surface area damaged, coating penetrated within 6 sec, substrate damage | 200 | 30 | Erosion failure |
| | | 15019 | 90% surface area damaged, coating penetrated within 6 sec, substrate damage, average depth of penetration 166 mils | 200 | 30 | Erosion failure |
| | | 15020 | 10% surface area damaged, surface cracks, subsurface fractures, damage initiated within 21 sec | 150 | 24 | Erosion damage |
| | | 15021 | 15% surface area damaged, coating penetrated, surface cracks, subsurface fracture, substrate damage, averaged depth of penetration 101 mills, damage initiated within 21 sec | 150 | 24 | Erosion failure |

Table 4. Phase I Test Results Summary (1 in.-hr rainfield, 2.0 mm raindrop, normal impact) (Continued)

| Priority | Material | AFWAL No. | Comments | Speed MPH | Duration sec | AFWAL/UDRI Category |
|---|---|---|---|---|---|---|
| 9 | FRCI-60-20/ .0738 #/Ft$^2$ SiC (CVD) (waterproofed) | 14917 | 40% surface area damaged, surface pitting, crater formation, average depth of penetration 75 mils, damage initiated within 24 sec | 200 | 30 | Erosion damage |
| | | 14918 | 30% surface area damaged, surface pitting, crater formation, damage initiated within 24 sec | 200 | 30 | Erosion damage |
| | | 14943 | 95% surface area damaged, coating penetrated within 6 sec, crater formation, channeling, substrate damage | 250 | 30 | Erosion failure |
| | | 14944 | 95% surface area damaged, coating penetrated within 6 sec, crater formation, channeling, substrate damage, average depth of penetration 273 mils | 250 | 30 | Erosion failure |
| | | 14919 | 10% surface area damaged, surface pitting, crater formation, average depth of penetration 35 mils | 150 | 30 | Erosion damage |
| | | 14920 | 5% surface area damaged, surface pitting, crater formation, average depth of penetration 35 mils | 150 | 30 | Erosion damage |

Table 4. Phase I Test Results Summary (1 in.-hr rainfield, 2.0 mm raindrop, normal impact) (Continued)

| Priority | Material | AFWAL No. | Comments | Speed MPH | Duration sec | AFWAL/UDRI Category |
|---|---|---|---|---|---|---|
| 10 | AETB-40-20/ .049 #/Ft$^2$ SiC (CVD) (waterproofed) | 14921 | 90% surface area damaged, coating penetrated within 6 sec, crater formation and channeling, substrate damage, average depth of penetration 116 mils | 200 | 30 | Erosion failure |
| | | 14922 | 90% surface areas damaged, coating penetrated within 6 sec, crater formation and channeling, substrate damage | 200 | 30 | Erosion failure |
| | | 14923 | 40% surface area damaged, surface pitting, crater formation | 150 | 24 | Erosion damage |
| | | 14924 | 50% surface area damaged, coating penetration within 18 sec, surface pitting, crater formation and channeling, average depth of penetration 52 mils | 150 | 24 | Erosion failure |

A test series with the samples oriented at 45 deg to the rain impact direction (Configuration 6, Figure 4) was also run using the RCG-coated FRCI-20-20 material. Results up to 250 mph for 60 sec time exposure indicate no damage. Because of a limitation on the available number of test samples, an undersized sample was also run at 300 mph. The sample was damaged, but since the damage was initiated at the lower tapered edge of the sample, which was especially exposed because of the small sample size, this result is highly suspect.

Pre- and post-exposure documentation of the surface condition, depth of penetration, and damage definition of all of the test articles was carried out under the supervision of Charles J. Hurley, University of Dayton Research Institute Aerospace Vehicle Coatings Group, and the negatives are on file with AFWAL/MLS. All of the test damage figures shown here are from that series of photographs.

1. RCG-Coated TPS

On the basis of the test results cited in Table 4, the damage threshold levels for the RCG-coated rigid tile materials have been evaluated and are summarized in Table 5. A 30-sec exposure duration in a 1-in. per hour rainfield is consistent with typical shuttle launch conditions if the launch were to occur through moderate rain. As was expected, the FRCI-20-20 with standard thickness RCG coating performed the best, surviving at 200 mph for 30 sec exposure with only the onset of subsurface fractures evident after the test (Figure 5). At 300 mph, the RCG coating was partially removed within 3 sec of exposure (Figure 6).

The onset of damage to the LI-2200 samples with the standard RCG coating thickness occurred around 150 mph after exposure for 60 sec, with appearance of an isolated star-shaped crack in one of the two exposed samples (Figure 7). At 200 mph, the RCG coating was penetrated and removed within a 12 to 18 sec exposure (Figure 8).

Damage to the FRCI-20-12 samples with standard RCG coating thickness was initiated within 21 sec at 150 mph, in the form of the removal of a small portion of the RCG coating (Figure 9) on one sample, and extensive subsurface microfracturing was noted on both samples after the run. The onset of damage

Table 5. Damage Threshold Levels (1 in./hr rainfield, 2.0 mm raindrop, normal impact)

| Priority | Material | Damage Threshold Speed mph/duration, sec |
|---|---|---|
| | **RCG-Coated and Waterproofed** | |
| 1 | FRCI-20-20 | 200/30 |
| 1a | LI-2200 | 150/60+ |
| 8 | FRCI-20-12 | < 150/21 |
| 1b | FRCI-20-12, 2x std. coating | 200/60+ |
| 1c | LI-900 | < 150/18 |
| | **RCG-Coated, Unwaterproofed and Filled With Water** | |
| 1d | FRCI-20-20 | 200/30 |
| | **Bare and Waterproofed** | |
| 5a | FRCI-20-20 | < 150/6 |
| 6 | LI-2200 | < 150/3 |
| 7 | FRCI-40-20 | < 150/9 |
| | **Bare, Underwaterproofed and Filled with Water** | |
| 5a | FRCI-20-20 | < 150/6 |
| | **SiC (CVD)-Coated and Waterproofed** | |
| 6b | LI-2200, 0.0234 lb/ft$^2$ coating | < 150/3 |
| 7a | FRCI-40-20, 2.5% coating | < 200/18 |
| 7b | FRCI-40-20, 0.0456 lb/ft$^2$ coating | 150/30 |
| 9 | FRCI-60-20, 0.0738 lb/ft$^2$ coating | 150/30 |
| 10 | AETB-40-20, 0.049 lb/ft$^2$ coating | < 150/18 |

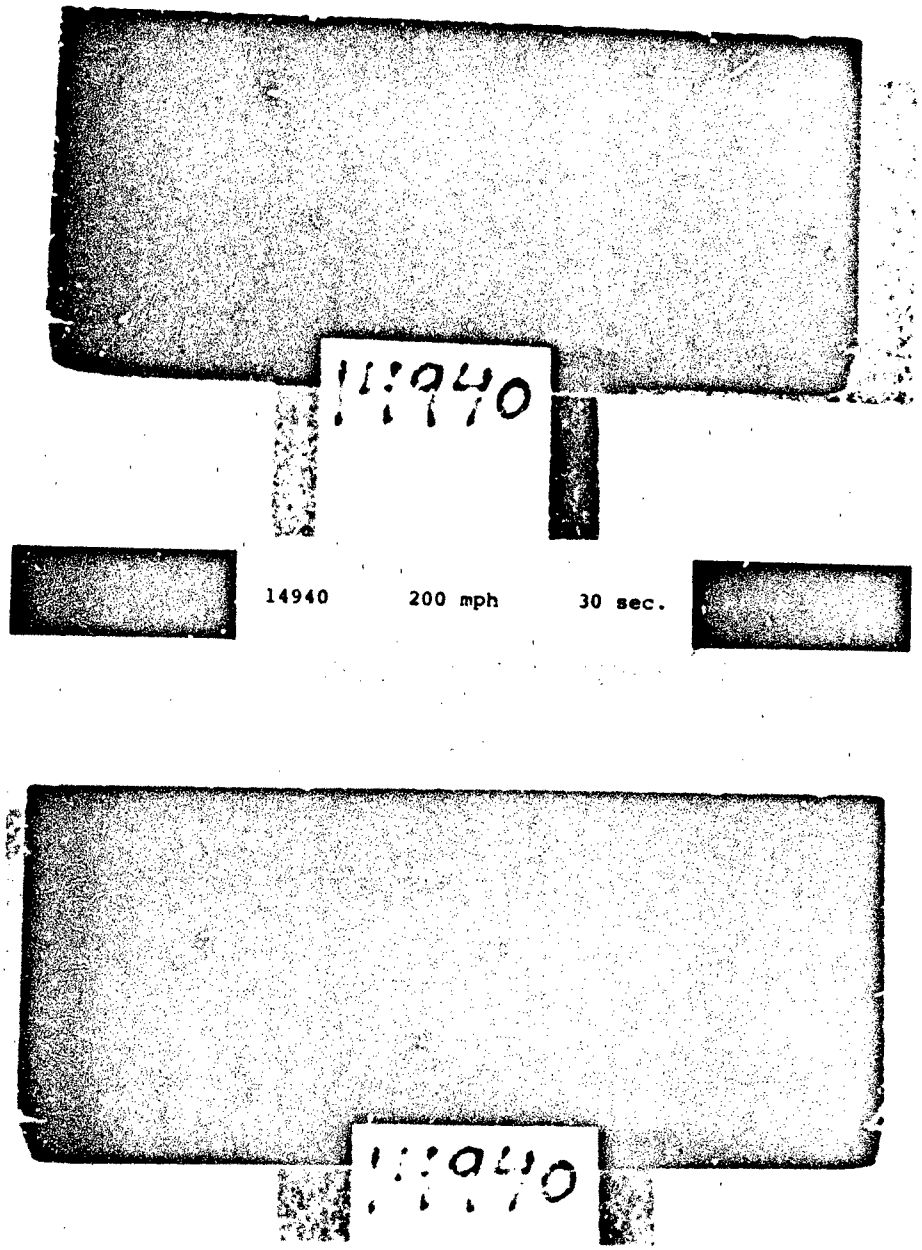


Fig. 5. Pre- and post exposure, FRCI-20-20 with standard RCG ceramic coating, showing subsurface fractures after 30 sec exposure at 200 mph

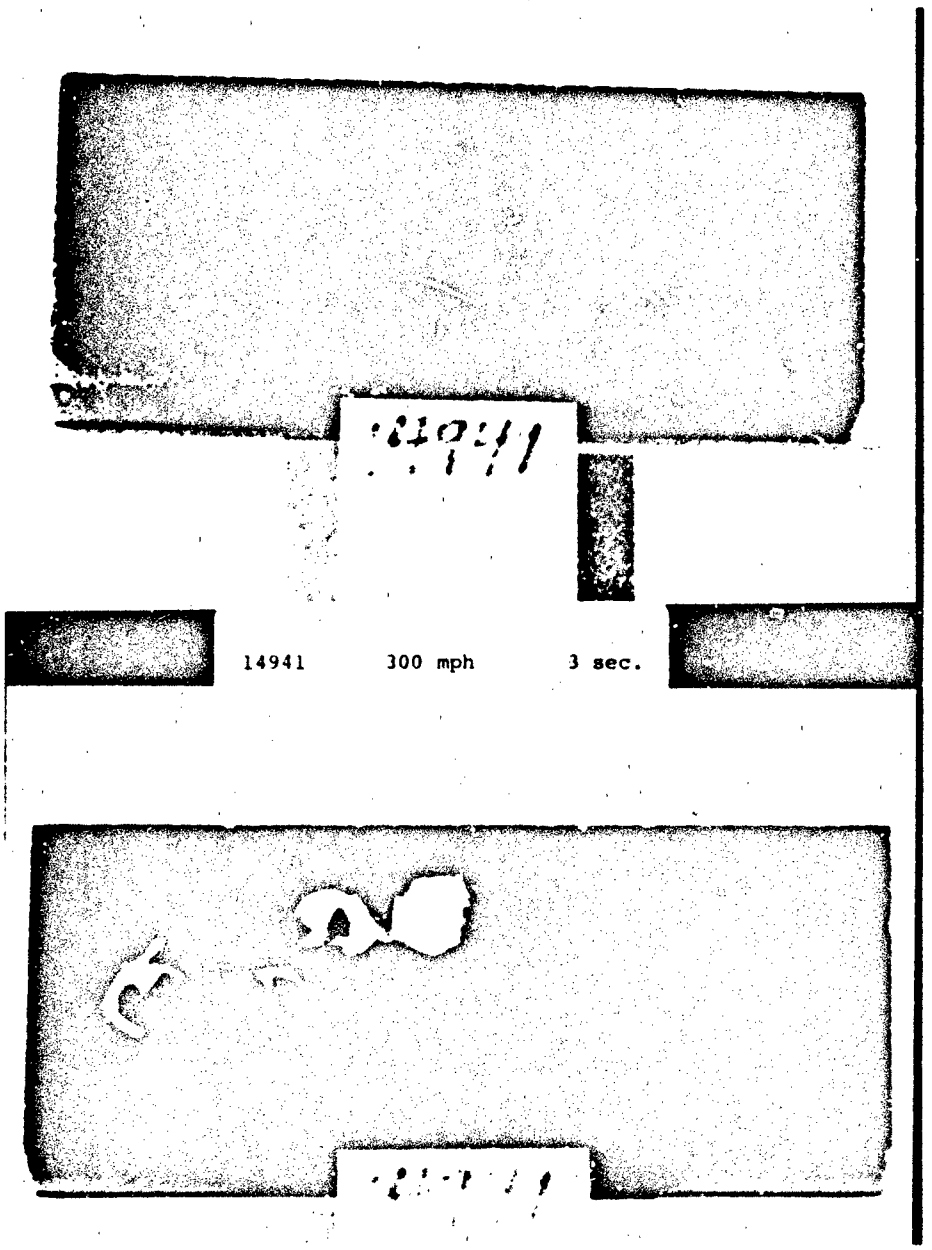


Fig. 6. Pre- and post exposure, FRCI-20-20 with standard RCG ceramic coating, showing damage after 3 sec exposure at 300 mph

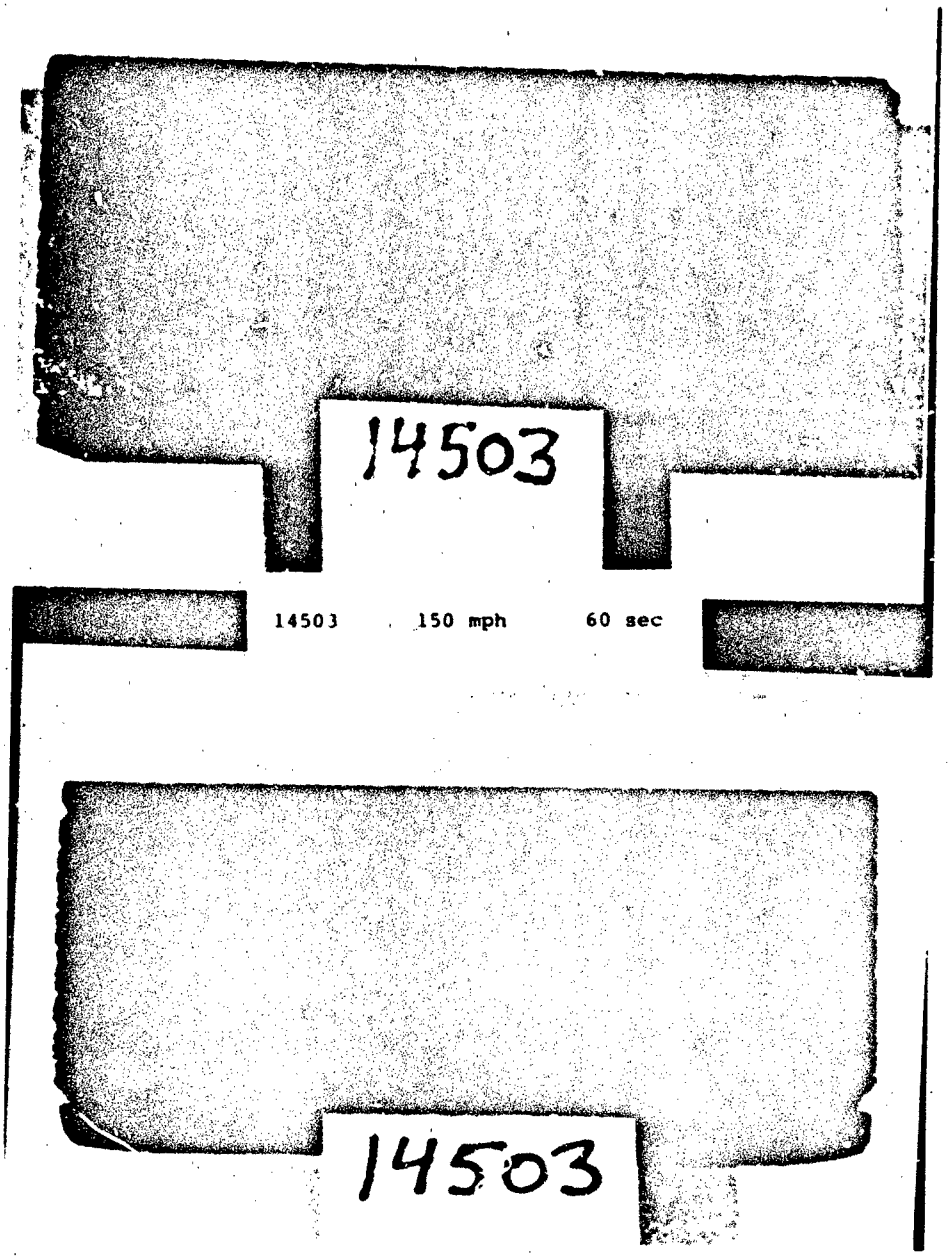


Fig. 7. Pre- and post exposure, LI-2200 with standard RCG ceramic coating, showing star-shaped crack after 60 sec exposure at 150 mph

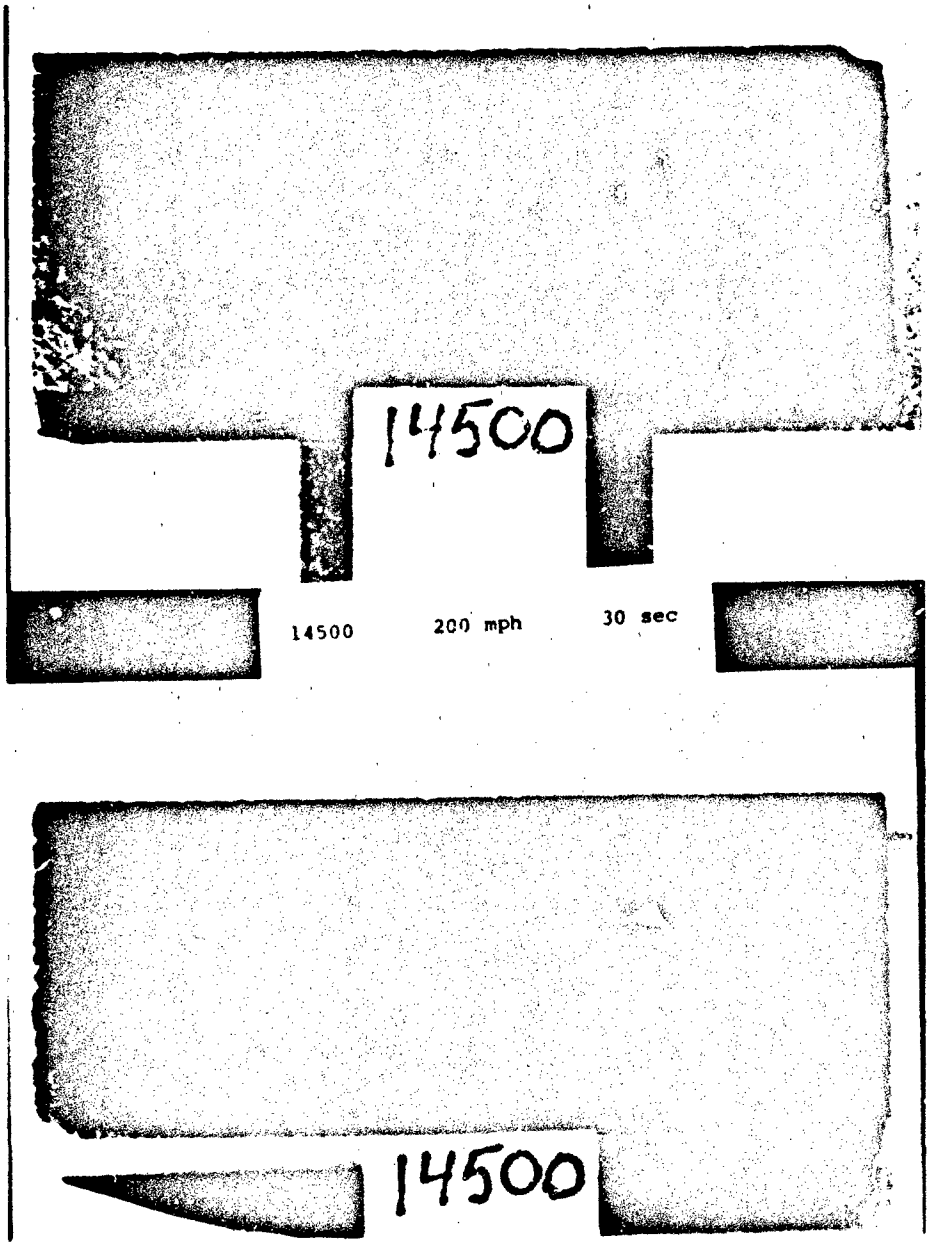


Fig. 8. Pre- and post exposure, LI-2200 with standard RCG ceramic coating, showing damage after 30 sec exposure at 200 mph

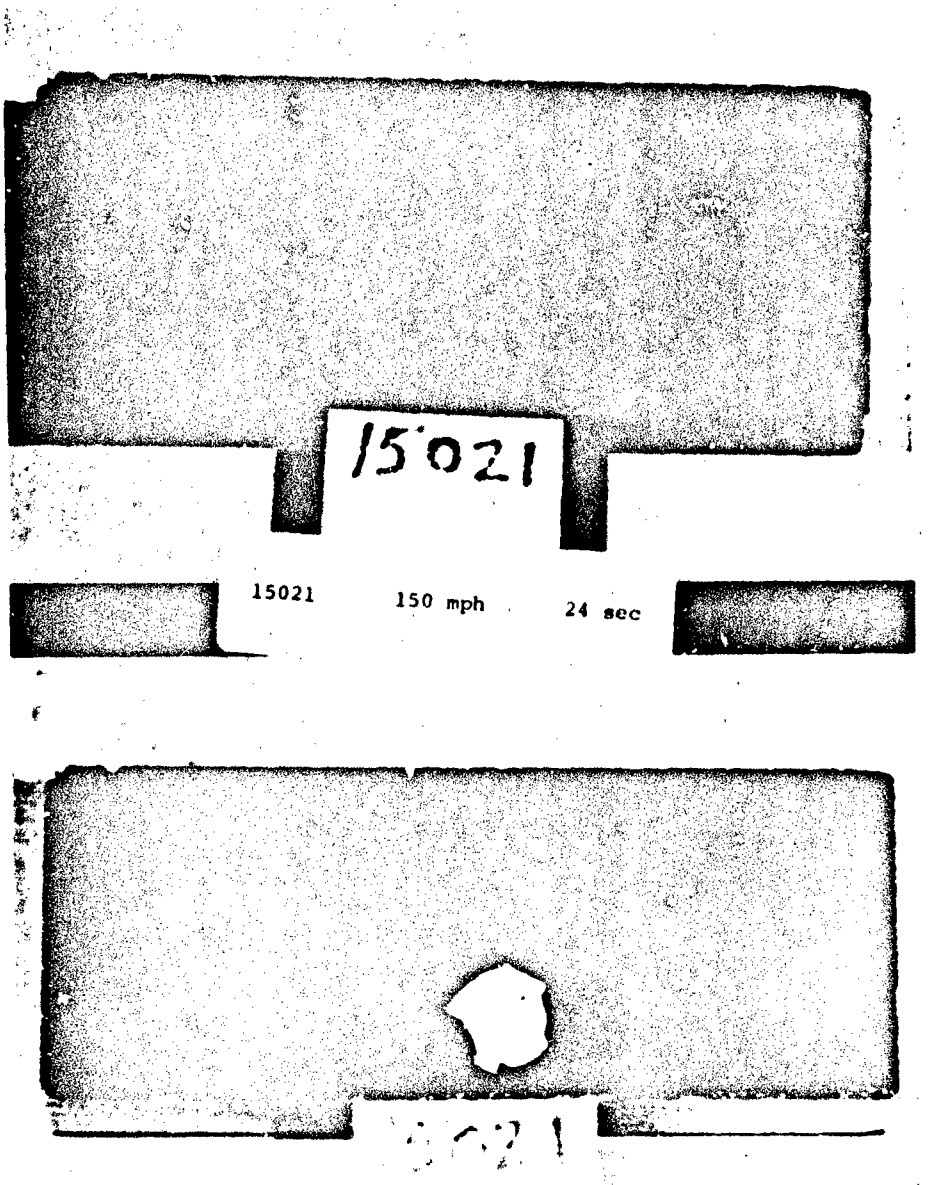


Fig. 9. Pre- and post exposure, FRCI-20-12 with standard RCG ceramic coating, showing surface cracks and loss of coating segment after 24 sec exposure at 150 mph

for a 30 sec duration would be expected at slightly below 150 mph. On the other hand, the FRCI-20-12 samples with twice the standard RCG coating thickness performed as well or slightly better than the FRCI-20-20 with standard coating thickness. At 200 mph, isolated fractures were found after 60 sec exposure time or longer in the case of FRCI-20-12 (Figure 10), whereas damage occurred within 30 sec in the case of the FRCI-20-20 with standard coating thickness.

For the LI-900 samples with the standard RCG coating thickness, portions of the coating were removed within 18 sec of exposure at 150 mph (Figure 11). At 200 mph, the coating was penetrated within 6 sec and the LI-900 tile substrate was eroded completely away at the inboard end of the samples. The damage threshold level for the LI-900 sample is estimated to be around 100 mph or less for a 30 sec exposure.

To investigate the possibility of anomalous results due to the takeup of water in the tile during the rain exposure run, one series of test samples (FRCI-20-20 with standard RCG coating thickness) was left unwaterproofed and each sample was filled by water immersion just prior to the test runs. Within the overall range of test result variations, there was no discernible difference in performance between the waterproofed and the "unwaterproofed and filled with water" test articles.

2. Uncoated Rigid Tile

All of the uncoated tile test articles were damaged by surface pitting and cratering at 150 mph test speeds. In the case of the bare waterproofed FRCI-20-20, the onset of surface pitting occurred 6 sec into the test run (Figure 12). Pitting was noted at around 9 sec into the 150 mph run of the bare, unwaterproofed and filled with water FRCI-20-20 samples. However, the accuracy within which these times can be determined is such that sample performance must be considered comparable between these two types of samples for this material. The bare, waterproofed LI-2200 material was pitted within 3 sec of exposure at 150 mph and the extent of the pitting appeared somewhat greater than that for the FRCI-20-20, which was exposed slightly longer (6 to 12 sec versus 3 sec). Surface pitting of the bare, waterproofed FRCI-40-20

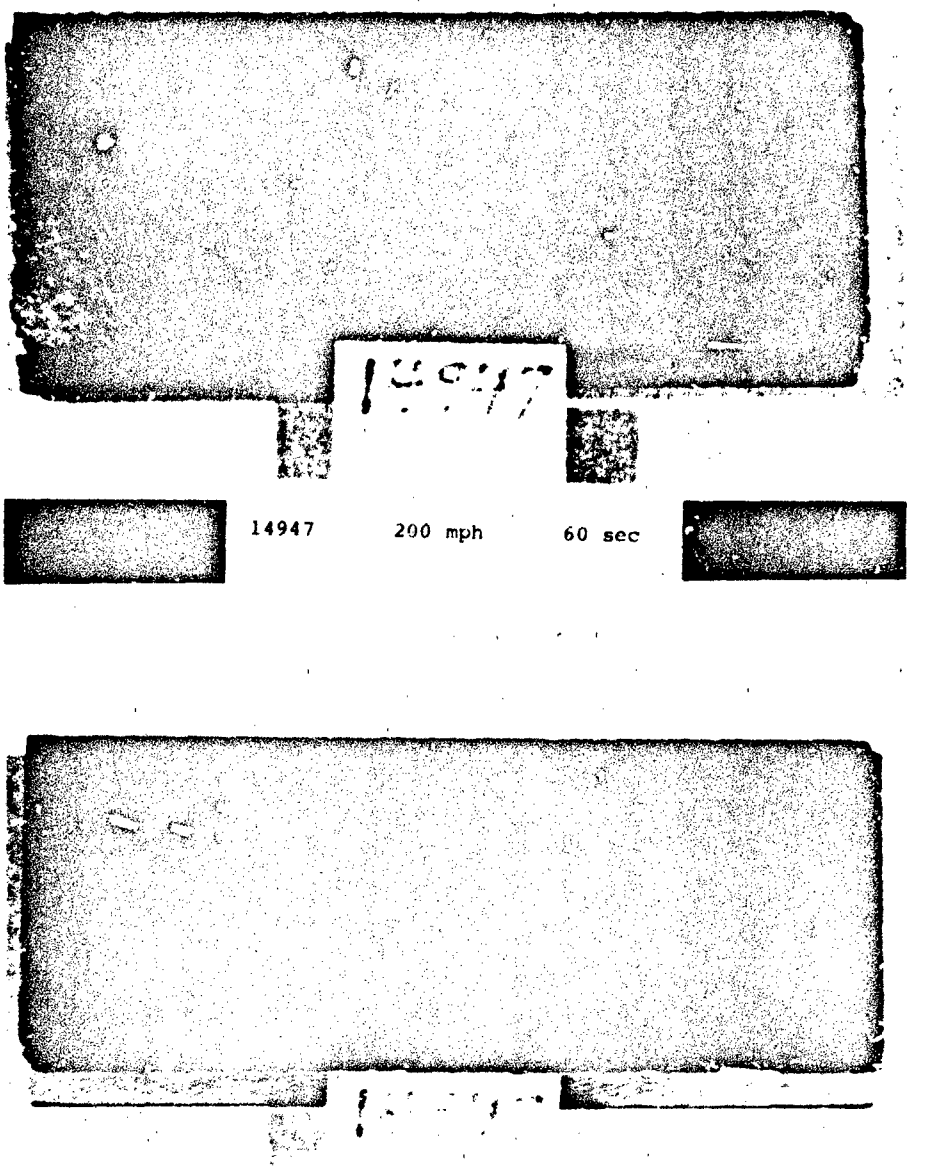


Fig. 10. Pre- and post exposure, FRCI-20-12 with twice standard thickness RCG ceramic coating, showing one subsurface fracture after 60 sec exposure at 200 mph

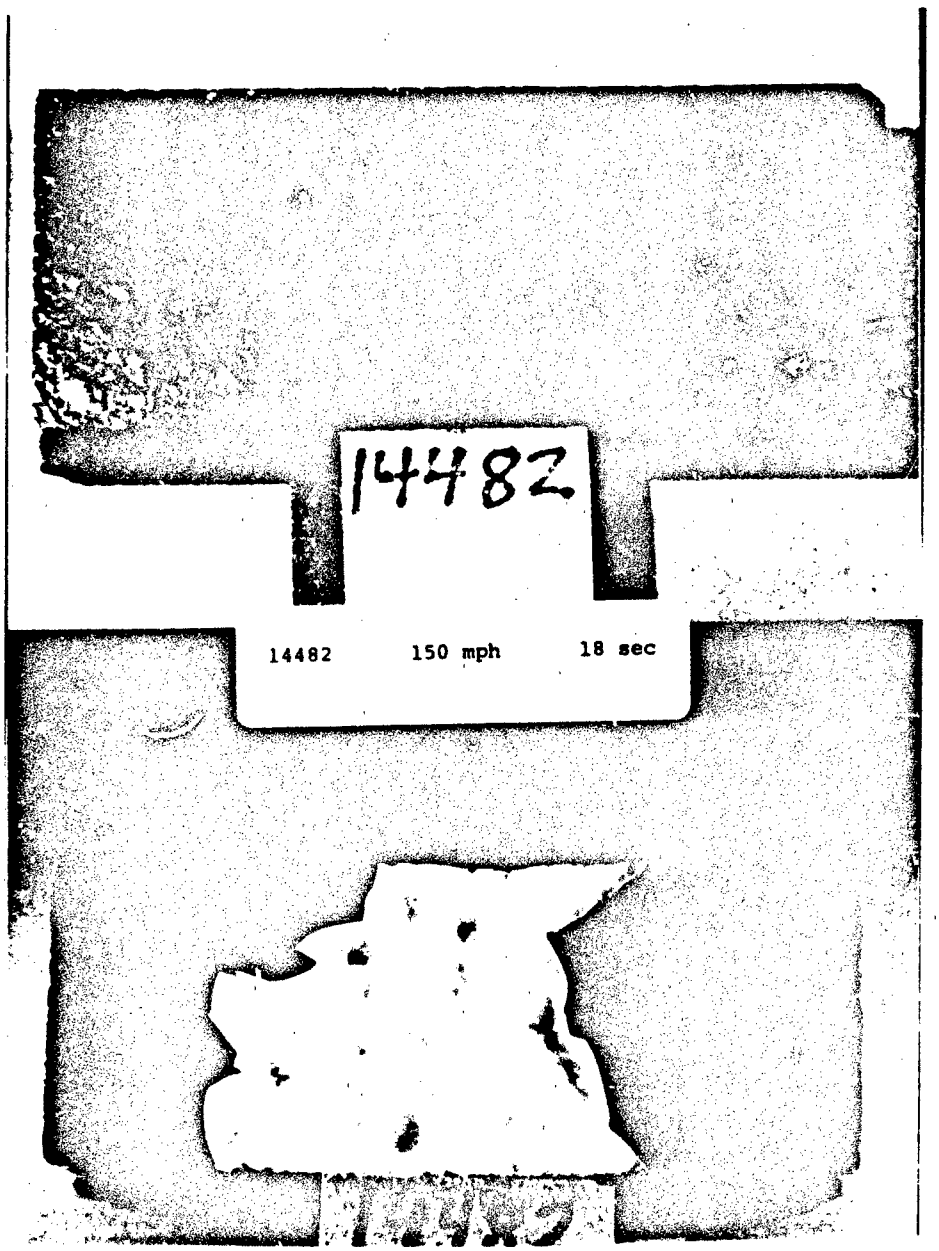


Fig. 11. Pre- and post exposure, LI-900 with standard RCG ceramic coating, showing ceramic coating loss and tile erosion after 18 sec exposure at 150 mph

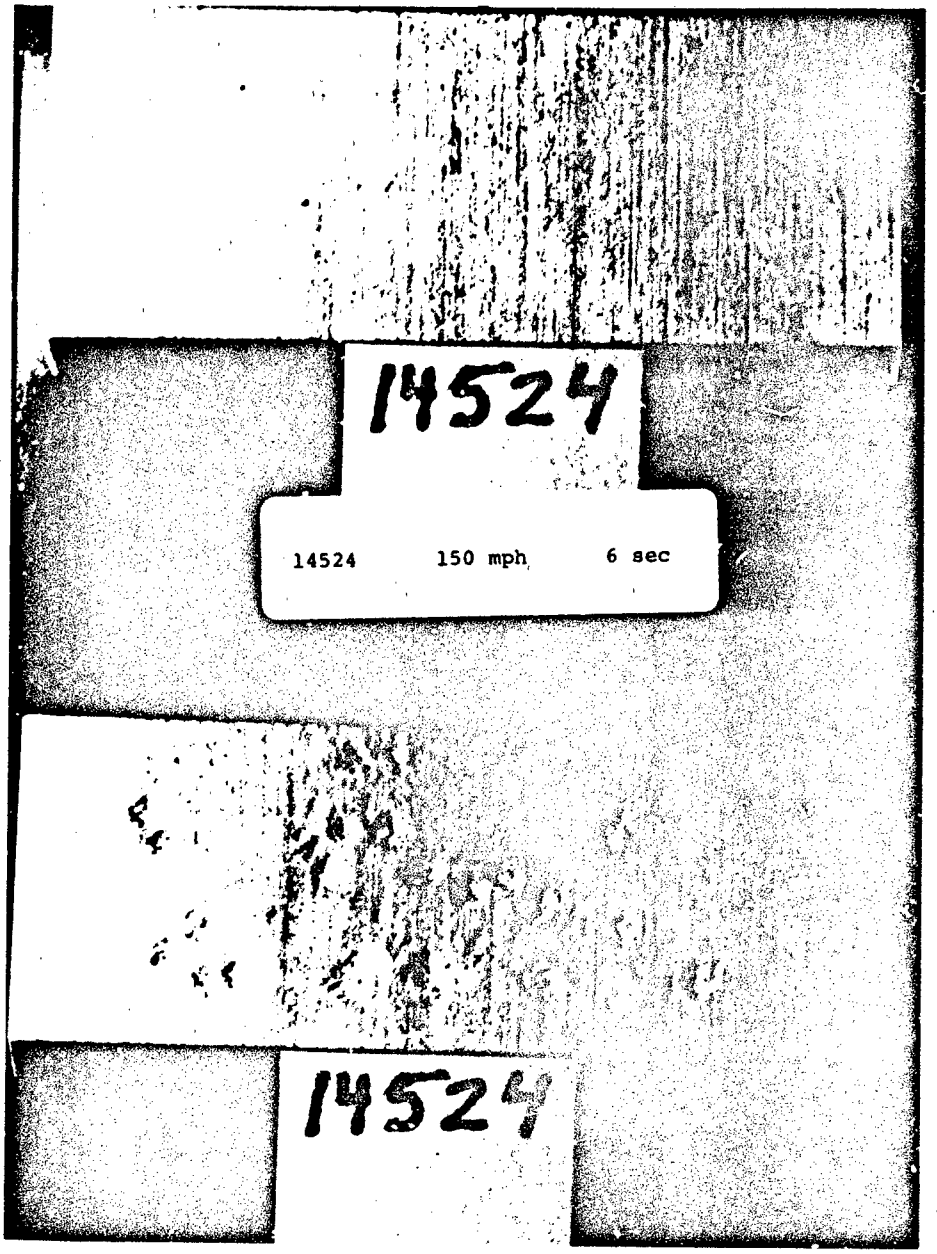


Fig. 12. Pre- and post exposure, FRCI-20-20, showing cratering after 6 sec exposure at 150 mph

test articles started at approximately the same time as noted for the FRCI-20-20 (i.e., approximately 9 sec into the run) at 150 mph, with the extent of the pitting also being comparable.

Thus, the damage threshold for all of the bare rigid tile materials tested is below 150 mph and could be considerably below that for a 30 sec exposure. As a means of evaluating the relative performance of the three uncoated materials tested (FRCI-20-20, LI-2200, and FRCI-40-20), the extent of the surface erosions produced by a 30 sec exposure at 200 mph was compared. Visual inspection of the test samples indicated that the depth of erosion of the LI-2200 samples is perceptibly deeper than that for the FRCI-20-20 and FRCI-40-20 samples. On a qualitative basis, it is difficult to establish a significant difference between the FRCI-20-20 and the FRCI-40-20.

It is concluded that the rain erosion resistance of the FRCI-20-20 and FRCI-40-20 class materials is generally superior to that of the LI-2200 material. However, the damage threshold levels for the three materials are less than 150 mph, possibly by a considerable margin for a 30 sec exposure.

3. SiC (CVD)-Coated TPS

A relative comparison of the SiC-coated test articles is more difficult than for the RCG coated test series because of the differences in coating thickness as well as changes in substrate tile material. Thus, the .0456 $lb/ft^2$ SiC coating on FRCI-40-20 (Figure 13) and the .1738 $lb/ft^2$ SiC coating in FRCI-60-20 appear to have a damage threshold level of around 150 mph for 30 sec exposure, although both experienced onset of surface pitting. Localized penetration and erosion of the LI-2200 tile with .0234 $lb/ft^2$ SiC coating occurred within 6 sec at 150 mph (Figure 14) and limited coating penetration occurred within 24 sec at 150 mph in the case of the AETB-40-20 with a 0.049 $lb/ft^2$ SiC coating.

It is very difficult to compare the different SiC-coated materials because of the mismatches in coating thickness and/or exposure conditions among the various test articles. It would appear that even fairly thick coatings experience the onset of pitting within 30 sec at 150 mph, but variations with coating thickness cannot be ascertained from the available data.

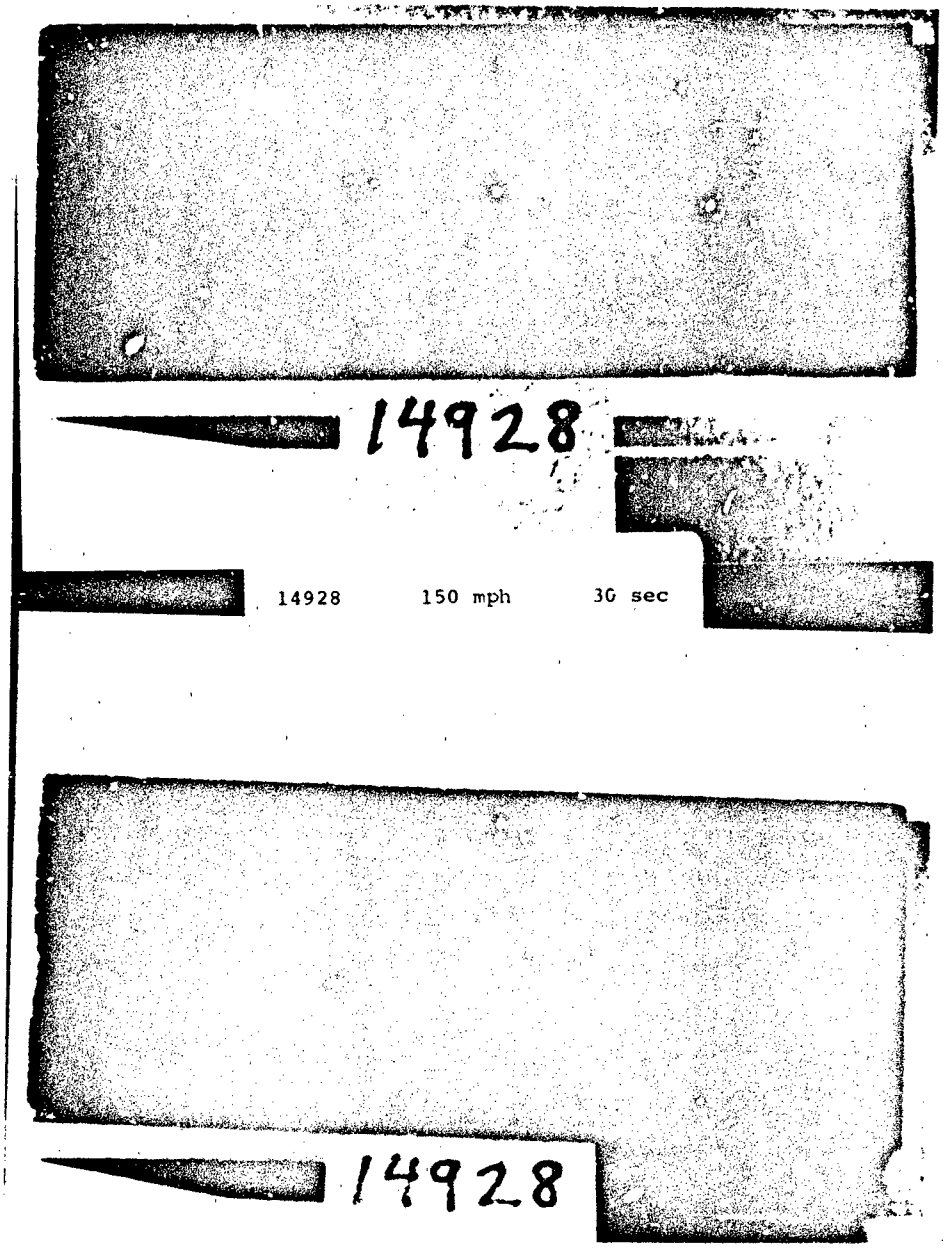


Fig. 13. Pre- and post exposure, FRCI-40-20 with 0.046 lb/ft$^2$ SiC (CVD) coating, showing cratering after 30 sec exposure at 150 mph

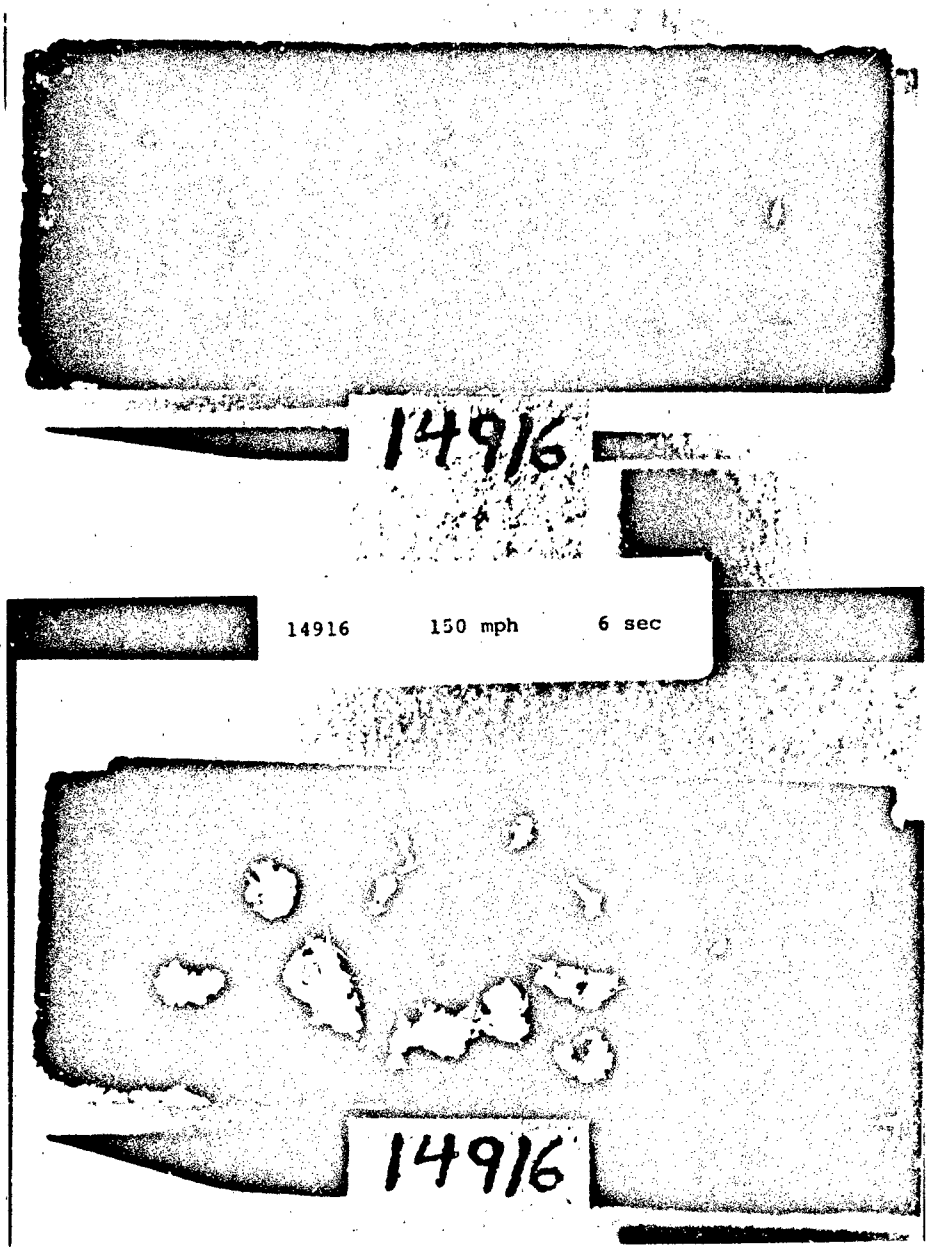


Fig. 14. Pre- and post exposure, Li-2200 with 0.023 lb/ft$^2$ SiC (CVD) coating, showing cratering and tile erosion after 6 sec exposure at 150 mph

4. Material Response

The damage observed in the thin RCG-coated tile materials differs from that seen in the uncoated and the SiC-coated configurations. Failure first occurs in the RCG ceramic coating in the form of subsurface microfractures at the interface between the coating and the porous tile substrate (Figure 15). In contrast, the SiC-coated materials and the bulk, uncoated tile materials fail by pitting and cratering of the surface layer. In all cases, erosion of the underlying porous tile material proceeds fairly rapidly after the surface coating or layer has been penetrated.

Damage progression in the RCG coating is characterized by propagation of the subsurface microfractures from the interface with the porous tile substrate to the surface, followed by the formation of star-shaped surface cracks and then the appearance of circumferential cracks around the star-shaped radial cracks. Coating segments are lost after the appearance of the radial and circumferential cracks. The various steps in this sequence can be seen in Figure 6, which shows an FRCI-20-20 sample after 3 sec exposure at 300 mph. Very similar results and observations have been noted by investigators at Rockwell International and by Varner (Ref. 7), who used metallic impactors to study tile damage.

The onset of damage to the CVD SiC coatings is characterized by the local fracturing of small chunks of SiC-impregnated surface materials over a small, roughly circular area apparently within a drop impact zone, which are initially driven into underlying voids. The fractured chunks remain within the underlying crater at most of the damage sites in the FRCI-40-20 and FRCI-60-20 samples exposed at the lowest test speed (150 mph for 30 sec; see Figure 13). The damage craters have sharp edges, suggesting a shear failure, in contrast to the classical lipped crater typically formed when metals are impacted. Sharp edged craters are also formed in the bare tile sample surfaces. The similar crater formation seen in the uncoated and CVD coated samples is not unexpected, since the CVD process represents an impregnation to some depth of the porous tile surface rather than the building up of a ceramic layer on the tile surface such as in the RCG ceramic coating case. When seen under mag-

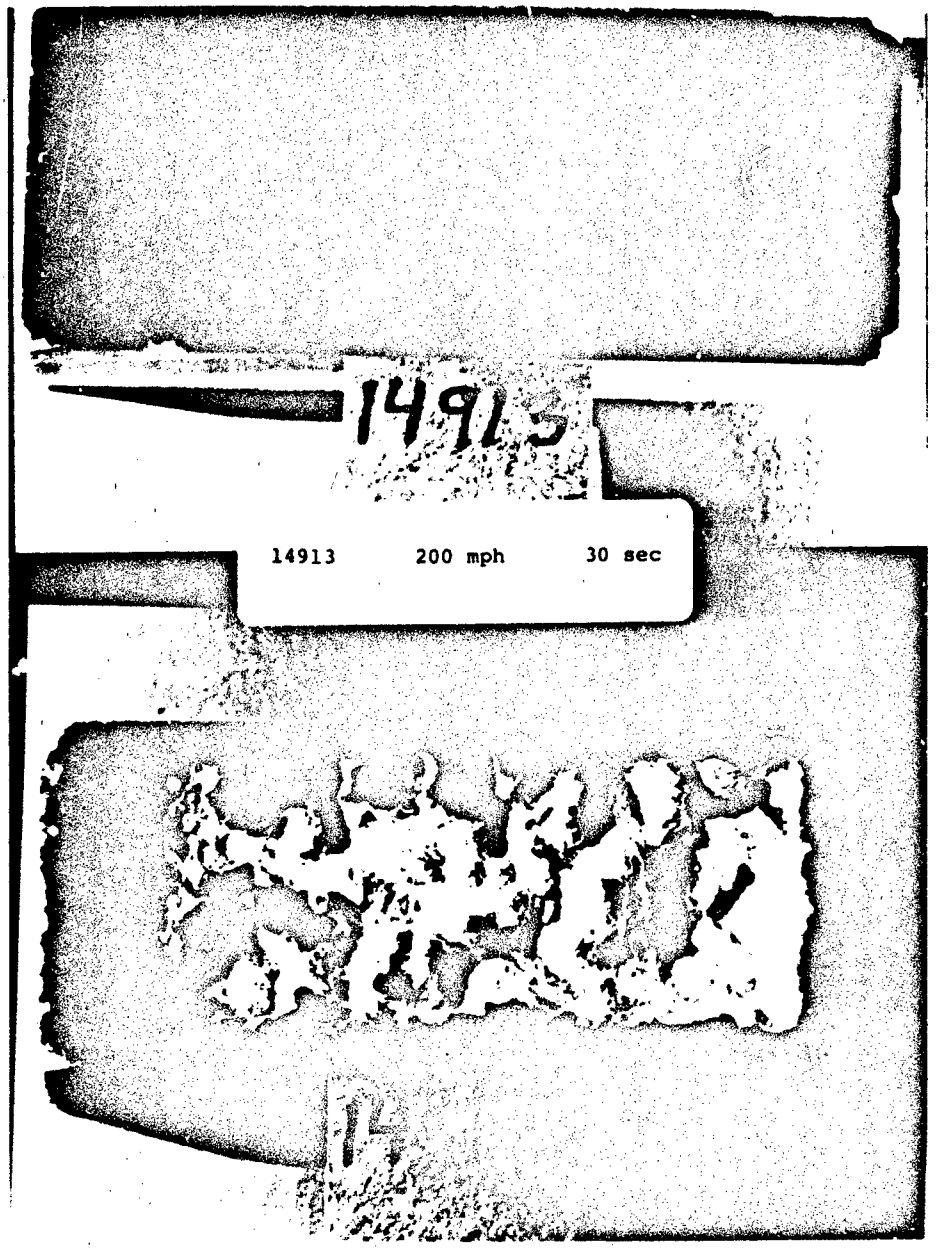


Fig. 15. Pre- and post exposure, LI-2200 with 0.023 lb/ft$^2$ SiC (CVD) coating, showing coating loss and tile erosion after 30 sec at 200 mph

nification, the FRCI-40-20 SiC coated sample surfaces have a straw-like appearance because the Nextel and Silica filaments making up the basic tile can still be seen even though impregnated with the SiC.

At higher speeds and/or longer exposure, the fractured SiC-impregnated surface chunks are ejected from the subsurface craters and underlying tile material is eroded to greater depths. There is no obvious indication that damage from one site is propagated to adjacent sites except where drop impact areas overlap, in contrast to the RCG ceramic response. Thus, damage progression in the uncoated and SiC-coated test articles mainly involves enlargement and deepening of surface craters only (compare Figures 14 and 15). One of the reasons for using CVD SiC coating was to strengthen the surface of the porous tile material, in addition to providing desired optical surface properties. The performance of the SiC-coated FRCI-40-20 suggests an improvement over the bare tile in rain impact resistance, and might warrant further exploration. However, there was virtually no difference in performance between the uncoated and SiC-coated LI-2200 test articles.

## C. DISCUSSION

The experimental evidence for the RCG coated tile samples indicates that failure is caused by flexure of the glass coating. At the lowest damage-inducing rain impact speeds, fractures visible through the glass coating are initially formed at the ceramic coating/porous tile interface. This has occurred in test articles exposed during the present test series in the AFWAL Mach 1.2 Rain Erosion Facility, and in samples exposed to the AFWAL/Bell Mach 3 Rain Facility, where larger (3 × 3 in.) test articles are used, during experiments carried out by Rockwell International experimenters on many of the same TPS candidate materials. At higher impact speeds or longer exposure durations, these subsurface microfractures propagate to the surface, eventually forming a radial (star) and circumferential crack system, followed by the removal of portions of the tile coating, thus exposing the underlying tile material to further erosion damage.

A NASA-sponsored study of the damage resistance of TPS tiles under single projectile impact, using an aluminum impactor and steel ball bearings (Ref. 7),

has produced similar results. Two types of damage were noted: (1) bending failure identical to that described above for the RCG ceramic coating, and (2) a Hertzian cone type impact failure (not obvious in the RCG ceramic coating failures of the Phase I tests).

A review of the literature indicates that most analyses of liquid drop impact of brittle (ceramic) materials (e.g., Ref. 8) consider the case of thick bulk meterials, generally modeled as occupying a half-space. The material damage threshold is assumed to be reached when preexisting surface microcracks are enlarged and extended by a tensile surface wave (the Raleigh wave) propagating out from the point of impact. A characteristic circumferential crack pattern is thus formed around the impact region, as has been shown experimentally (see Figure 11, Ref. 9, for example). Some of the damage produced in the RCG ceramic coating by ball bearing experiments discussed in Ref. 7 (referred to as the impact failure case) seems similar to the circumferential or ring cracking modes shown in Ref. 9.

These considerations indicate that there may be at least two damage modes involved in producing failure of the rigid TPS under rain impact conditions: (1) bending of the ceramic coating resulting in tensile failure at the interface with the porous tile substrate, and (2) cratering of the surface because of shallow tensile surface waves interacting with preexisting surface microcracks. In the case of the very thin ceramic RCG coating presently used on the TPS, the flexural failure is apparently reached at lower raindrop impact speeds than are needed to cause the surface cratering type damage in the coating. However, if the thickness of the ceramic coating is increased, the increased flexural stiffness of the coating could result in a shift of the failure sites to the surface by the shallow tensile surface wave interaction with existing surface microcracks.

After the initial subsurface fractures in the ceramic coating have propagated to the surface, some of the bulk material cratering mechanisms, particularly hydraulic penetration into the fracture network and jetting of water drop outflow against elevated crack edges in irregular crater contours, could also come into play. That is, once the coating damage threshold has

been exceeded, fracture propagation mechanisms common to both thin and thick (bulk) ceramic layers can be expected.

The pitting or crater-type failure of the bare and CVD SiC-coated test specimens may be related to the "impact failure" damage mode characterized in Ref. 7, although the SiC surface fragments or chunks remaining in the impact craters are generally not circular but irregular in shape. Differences in projectile breakup (i.e., raindrop breakup in the present experiments versus no breakup of the impacting steel ball bearings in the Ref. 7 experiments) could also lead to differences in tile response.

A very interesting paper by G. Schmitt (Ref. 10) provides data for thin skin composite structures which include a configuration analogous to the rigid TPS under discussion. Of particular interest is a composite with an outer skin of 10- to 30- mil thick E-glass/epoxy over rigidized, expanded, low density polyurethane foam. Polyurethane or fluorocarbon protective coatings were applied to the outer skin to improve rain impact resistance. The core density varied from 5 to 15 $lb/ft^3$, i.e., roughly in the same range as for the current TPS substrate materials, and the outer skin thicknesses were also comparable to the RCG ceramic coating thickness.

At or below a certain thickness of outer skin (20 mil or less) no amount of protective coating or core (substrate) density change improved performance; failure was almost instantaneous, with separation of the outer skin from the foam and possibly some crushing of the foam. Inter-ply delamination of the laminated outer skin also was common. With an increase in outer skin thickness to 30 mils, however, there was a marked improvement in time-to-failure with increase in expanded foam core density for exposure at 400 mph in a 1-in.per/hr rainfield. Part of the improved performance may be attributable to the high strain-to-failure ratio, which is characteristic of the E-glass layer, as opposed to the brittle RCG coating on our tile specimens.

Thus, while it was concluded in Ref. 10 that the density of the core (substrate) material was the most significant materials parameter in achieving rain impact resistance, it was also necessary to have a sufficiently thick outer skin before substantial improvement was achieved with increased substrate density.

The results of the present experiment appear to be consistent with the trends suggested in Ref. 10. Increases in tile substrate density for the same generic materials class seemed to increase rain impact resistance; an increase in ceramic coating thickness likewise resulted in improved impact performance.

The role of the tile substrate material is obviously of primary importance in determining TPS rain impact performance. Key material properties would appear to include density, porosity, compressive strength, and compressive modulus. Some typical physical and mechanical properties of the tested tile materials are given in Table 6. The tiles are listed in the order of relative performance, beginning with the worst (LI-900) and proceeding to the best (FRCI-20-20). The strongest correlation with improved performance appears to be shown by the through-the-thickness (TTT) compressive modulus. The density of LI-2200 is slightly higher than that for the FRCI-20-20, but its performance is inferior to that of the FRCI-20-20. Similarly, FRCI-20-12 and LI-2200 have the same compressive strength, but the LI-2200 performance is definitely superior to the FRCI-20-12.

Table 6. Typical Physical and Mechanical Properties

| Property | LI-900 | FRCI-20-12 | LI-2200 | FRCI-20-20 |
|---|---|---|---|---|
| Density, $g/cm^3$ | 0.14 | 0.19 | 0.35 | 0.32 |
| Compressive Strength, psi | 28 | 132 | 130 | 250 |
| Compressive Modulus, (TTT) $10^4$ psi | 0.7 | 1.05 | 2.7 | 3.7 |
| Sound Speed, $10^5$ cm/sec | 0.59 | 0.58 | 0.73 | 0.89 |
| Acoustic Impedance $10^5 g/cm^2$ sec | 0.08 | 0.12 | 0.26 | 0.29 |

If the RCG-coated TPS materials can be modeled as the classical beam or plate on an elastic foundation, with the tile substrate providing the foundation modulus for the thin ceramic "plate," then the tile compressive modulus becomes a key parameter in the reaction between the coating and the tile. However, the peak bending stress in the beam or plate is not very sensitive to the modulus of the foundation (Ref. 11). From the analysis of a railroad track rail, a 100% change in the foundation modulus only produces a 16.5% change in the maximum bending stress in the rail (Ref. 11, p 28). On this basis, the difference in compression moduli for the tile test materials would not be expected to cause a wide variation in damage threshold levels.

As discussed in Appendix A, the pressure loading on the TPS surface during a raindrop impact at 200 mph is on the order of 16 ksi, based on the water hammer pressure (Ref. 9) and typical materials properties for water and the RCG coating. For a 2.0 mm drop diameter, the pressure duration is between 1 and 2.5 μsec. The acoustic impedance mismatch at the RCG ceramic coating/tile substrate interface is also large, so that very little stress is transmitted into the substrate from the initial stress wave produced at the surface by the raindrop impact. Flexure of the RCG coating is probably well developed before the end of the pressure loading, however, because of the short travel time (approximately 0.07 μsec) for a stress wave to traverse the thickness of the 0.38 mm (15 mil) coating. A reduction in the acoustic impedance mismatch between the RCG coating and the tile substrate would allow more of the impulsive-like loading to be taken up in the substrate and might also reduce the subsequent flexural motion of the coating, thus reducing the flexural stress in the coating and leading to improved rain impact resistance.

## VI. CONCLUSIONS AND RECOMMENDATIONS

The Phase I testing was successful in bracketing damage threshold levels for three of the RCG-coated test materials (LI-2200, FRCI-20-20, and FRCI-20-12 having twice the standard 15 mil coating thickness). The damage threshold level was found to be less than 150 mph for LI-900 and FRCI-20-12 with standard coating thickness, and the bare tile materials (LI-2200, LI-900, FRCI-20-12, FRCI-20-20, and FRCI-40-20). The CVD SiC-coated test articles (LI-2200, FRCI-40-20, FRCI-60-20, and AETB-40-20) failed at or below 150 mph under 30 sec exposure durations. Difficulties with the testing technique precluded valid test data on the flexible cloth layers because of complications arising from cloth layer mounting constraints and coupling between sample distortion and centrifugal force loads on the test samples. Alternatives to the present approach are needed to provide valid test data on the flexible blanket class of materials.

Damage to the RCG-coated tiles is initiated by flexural bending stresses in the ceramic coating; similar behavior was reported for tests using larger test samples on the Mach 3 AFWAL/Bell facility and also for drop tests using an aluminum cylinder with a hemispherical head as an impactor.

The relative ranking of the rigid TPS materials with a standard thickness RCG ceramic coating in regard to rain impact resistance is:

FRCI-20-20 (best)
LI-2200
FRCI-20-12
LI-900 (worst)

The compressive modulus of the material appears to correlate most strongly with the rain impact resistance of the RCG-coated tile specimens. Although there is a considerable spread in the compressive modulus properties between the several materials, there is no dramatic improvement in damage threshold speeds from the weakest (LI-900) to the strongest (FRCI-20-20) material, i.e., from somewhat under 150 to 200 mph. This could perhaps have

been anticipated from the analogy with the railroad track rail on an elastic foundation, cited above.

The performance of the bare tile material does not appear to be substantially improved by infiltration, impregnation and sintering using CVD SiC on the tile surface. While there was some improvement in rain impact resistance of the FRCI-40-20 material, there was no change in the case of the LI-2200.

Finally, the rain impact resistance of the FRCI-20-12 was substantially improved by doubling the thickness of the RCG ceramic coating. This result could be expected because of the increased flexural stiffness of the ceramic coating and the role of the flexural failure modes in determining damage threshold.

Future studies are recommended to examine the role of impact angle of incidence in determining damage threshold levels under more realistic or operational rain encounter conditions (as opposed to the 90 deg, normal impact angle studied here).

It is also recommended that improved rain resistance be studied by use of tile substrate surface hardening techniques such as CVD SiC infiltration or the shuttle tile densification technique combined with application of the standard RCG ceramic coating. The limits to which impact resistance is improved by increasing the RCG ceramic coating thickness should also be established. Trade-off studies between improved rain impact performance and weight penalty will require such data.

To establish a better understanding of the relative importance of various materials properties, another series of experiments is recommended with the same basic tile materials, but two and three times the standard RCG ceramic coating thickness, to see if more dramatic improvements in rain impact resistance are achievable with increase in compressive modulus or tile density, as was the case in Ref. 11. The test matrix should provide for a tighter variation in test duration at a given test velocity than was possible in Phase I, in calling out specific velocities and durations to determine damage initiation, damage propagation, and rate of damage onset.

## REFERENCES


1. Wahl, N. E. Rain Erosion Characterization of Thermal Protection System Materials at Subsonic Velocities, AFML-TR-72-145. Air Force Materials Laboratory, Wright-Patterson Air Force Base Ohio, Aug. 1972.

2. Stein, M. and R. C. Ketterer, Reuseable Surface Insulation Flight Environment Test Program. NASA/KSC Engineering and Rockwell International Launch Operations, Florida. Interim Report, 18 July 1975, Final Report, Dec. 1976.

3. Teller, V., D. Cade, and P. DeWolfe, "Ice Impact Testing of Orbiter TPS Materials Progress Report," Operational Design Projects, Rockwell International, December 1982 (Briefing).

4. Hurley, C. J. and G. F. Schmitt, Jr., Development and Calibration of a Mach 1.2 Rain Erosion Test Apparatus, AFML-TR-70-240, Air Force Materials Laboratory, Wright-Patterson AFB, Ohio 45433, Oct. 1970.

5. Schmitt, G. F., Jr., Liquid and Solid Particle Impact Erosion, AFML-TR-79-4122, Air Force Materials Laboratory, Wright-Patterson Air Force Base, Ohio 45433, Nov. 1979.

6. Hackworth, J. V., "A Mechanistic Investigation of the Rain Erosion of Infrared Transmitting Materials at Velocities to Mach 2", Proc. 5th Int. Conf. on Erosion by Solid and Liquid Impact, pp 10-1 to 10-12, Cambridge, England, Royal Aircraft Establishment, Farnborough, England, 3-6 September 1979.

7. Varner, J. R. and K. Ono, Damage Resistance of Space Shuttle Orbiter Thermal Protection Tiles, Final Report, Interchange No. NCA2-OR390-901, 1979, NASA Ames Research Center, Moffett Field, California. 1979.

8. Evans, A. G., Y. M. Ito, and M. Rosenblatt, "Impact Damage Thresholds in Brittle Materials Impacted by Water Drops," Proc. 5th Int. Conf. on Erosion by Solid and Liquid Impact, 3-1 to 3-10, 1979.

9. Adler, W. F., "Rain Erosion Mechanisms for Optical Materials," Optics in Adverse Environments, Vol. 21, SPIE Proc. (1977).

10. Schmitt, G. F., Jr., "The Subsonic Rain Erosion Response of Composite and Honeycomb Structures," SAMPE Journal, September/October, pp. 6-13, 1979.

11. Hetényi, M., Beams on Elastic Foundation, The University of Michigan Press, Ann Arbor, Michigan, 1958.

## APPENDIX A. THEORETICAL CONSIDERATIONS

The magnitude and spatial distribution of the pressure exerted on a solid surface by a liquid drop impact is a complex function of time, requiring hydrodynamic calculations using numerical techniques for accurate determination (Refs. 8 and 9). For the purpose of this discussion, the magnitude of the pressure can be estimated from the water hammer pressure equation:

$$p = \frac{\rho_L c_L}{1 + (\rho_L c_L / \rho_c c_c)} V \tag{1}$$

where $\rho$ is density, c is sound speed, V is the raindrop impact speed (normal to the surface), and the subscripts L and c refer to liquid and surface coating, respectively. The product $\rho c$ is called the acoustic impedance,

$$Z = \rho c \tag{2}$$

Equation (1) is rewritten in terms of the acoustic impedance

$$p = \frac{Z_L}{1 + (Z_L / Z_c)} V \tag{3}$$

An upper limit for the duration of the impact pressure loading is given by

$$t_L = \frac{2d}{c_L} \tag{4}$$

which is the time required for a compressional stress wave to reach the rear surface of a raindrop of diameter d and reflect back to the impact surface as a tensile, unloading wave. The sequence of events involved in a raindrop collision with a plane surface is more complicated than is indicated by such a simple wave passage model. Of particular importance is lateral outflow of the liquid as the raindrop area of contact with the surface increases (Ref. 9).

The transit time of a stress wave through the thickness direction of a TPS coating is

$$t_c = \frac{h}{c_c} \tag{3}$$

where h is the coating thickness and $c_c$ is the sound speed in the coating material.

For analysis, the following materials properties have been assumed for estimating raindrop impact of an RCG-coated FRCI-20-12 tile specimen:

Table A-1. Assumed Acoustic Impedance Properties

| Material | $\rho$ Density, $g/cm^3$ | c Sound Speed $10^5$ cm/sec | Z Impedance $10^5 g/cm^2$ sec |
|---|---|---|---|
| Water | 1.0 ($\rho_L$) | 1.46 ($c_c$) | 1.46 ($Z_L$) |
| RCG Coating | 1.69 ($\rho_c$) | 4.0 ($c_c$) | 6.83 ($Z_c$) |
| RSI Nominal (12#/ft$^3$) | 0.19 ($\rho_s$) | 0.58 ($c_s$) | 0.12 ($Z_s$) |
| Meas.* | 0.215 | 0.456 | 0.098 |

*Sound speed measurements provided by J. Linn, The Aerospace Corporation.

From Eq. (3) and the properties assumed in Table A-1, the water hammer pressure has been calculated as a function of raindrop impact speed and is plotted in Figure A-1. The pressure is in the range from 0.8 to 1.6 kbar for impact speeds in the range of the present experiments, i.e., from 150 to 300 mph. Since typical static compressive strengths of borosilicate glasses are on the order of 8.4 kbar (Ref. A-1), the Phase I test speeds do not appear

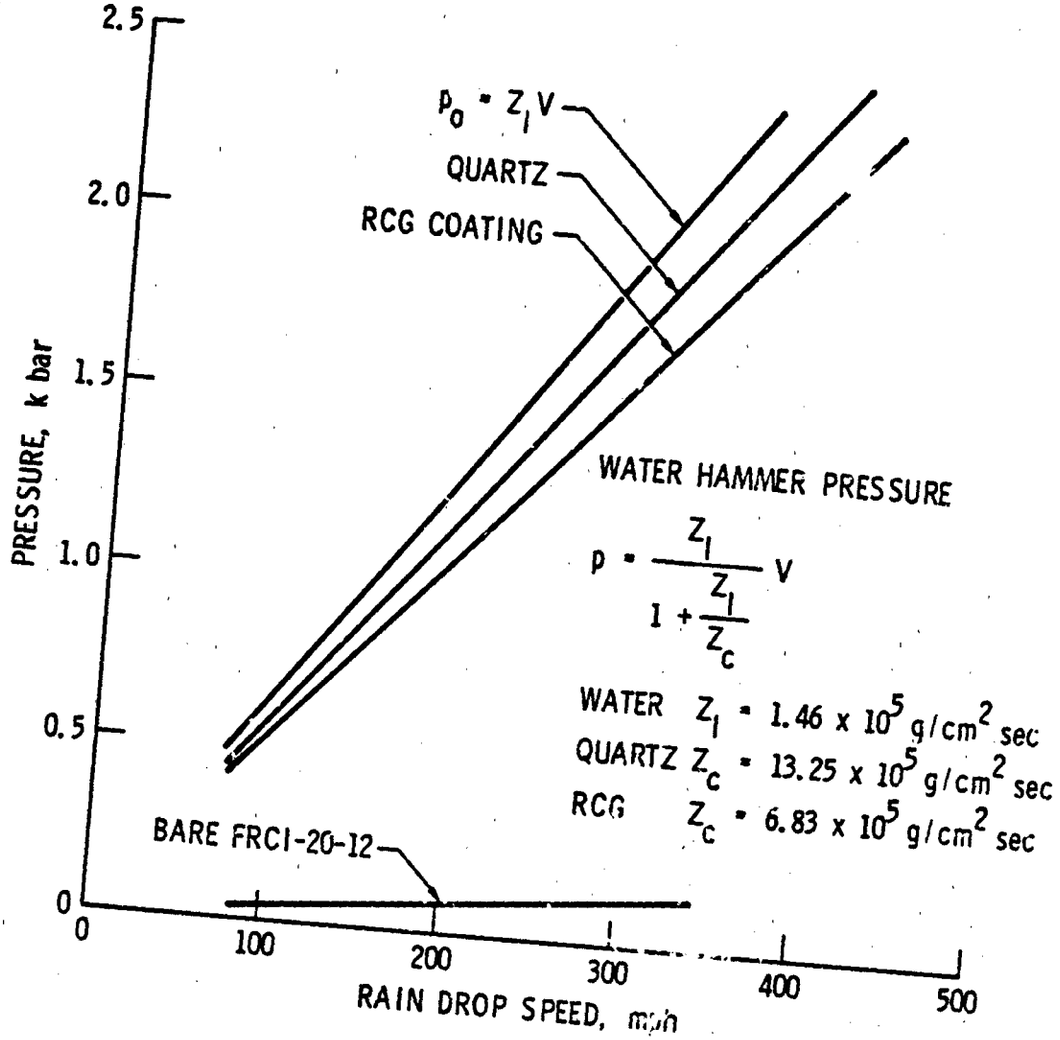


Fig. A-1. Water hammer pressure as a function of raindrop impact speed

to be high enough to produce gross crushing or pulverizing damage to the RCG coating surface from compressional loading. The surface damage to bulk silicate-based glasses reported in Ref. 9 was initiated by impact pressures on the order of 3 kbars, at speeds of around 500 mph. In Ref. 8, the onset of surface damage is attributed to the propagation of pre-existing surface cracks caused by the tensile pulse associated with the Rayleigh surface wave that emanates from the impact site on a bulk specimen.

On the basis of estimated magnitudes of the raindrop impact pressure loadings, it seems reasonable to conclude that the dominant failure mechanism in the RCG-coated TPS specimens was coating flexure and not surface cratering in the coating. From Eq. (4), an upper limit on the pulse duration for a 2.0 mm diameter raindrop is

$$t_L = 2.5 \ \mu\text{sec}$$

From Ref. 9, it is estimated that for such a case, the impact event is completed in approximately 1 μsec. From Eq. (5), the transit time for a stress wave to propagate through a standard thickness RCG coating (0.38 mm) is

$$t_c = 0.07 \ \mu\text{sec}$$

Thus, since the pressure pulse duration is in the range from 1 to 2.5 μsec, it is long compared to the transit time through the coating, and flexural motion of the coating is probably well developed before the end of the pressure loading from a single raindrop impact.

During very early times after a raindrop impact, before the flexural response of the coating has been excited, the magnitude of the initial stress wave transmitted into the tile substrate, $\sigma_s$, can be estimated from the relation (Ref. A-2)

$$\frac{\sigma_s}{\sigma_c} = 1 + \frac{Z_s - Z_c}{Z_s + Z_c} \qquad (6)$$

where $\sigma_c$ is the magnitude of the stress induced in the coating, assumed here to be water hammer pressure developed upon raindrop impact of the coating. Taking the values for the acoustic impedance from Table A-1, Eq. (6) yields

$$\frac{\sigma_s}{\sigma_c} = 0.028$$

Thus, because of the large impedance mismatch ($Z_c >> Z_s$) between the RCG coating, and the FRCI-20-12 substrate, the interface between the coating and the tile almost appears to be a free surface to the initial stress wave in the RCG coating and very low stress amplitudes are transmitted into the substrate.

Equation (6) is based upon the assumption that the coating and substrate materials are continuous, homogeneous, elastic materials. Consequently, the application of the relation to porous tile materials is only approximate, but still provides some insight into likely responsive behavior early in the impact event.

In the same fashion, an approximate estimate of the pressure loading imposed upon a bare tile specimen by raindrop impact can be made using Eq. (3), which likewise is valid only for continuous, homogeneous materials. Consequently, the results can only be regarded as order of magnitude values. Using $Z_s$ in place of $Z_c$ in Eq. (3) yields

$$p = 0.41 \times 10^{-3} \text{ V(in mph), kbar}$$

For an impact speed of 150 mph, p = 0.062 kbar. Since the static compressive strength of FRCI-20-12 is on the order of 0.008 kbar, surface crushing would be expected, as was observed during the Phase I tests.

## REFERENCES


A-1. Morey, G. W., The Properties of Glass, 2nd Edition, Reinhold Publishing Corporation, New York, New York, 1960.

A-2. Kinslow, R., Stress Waves in Composite Laminates, AEDC-TR-65-69, 1965, ARO, Inc., Arnold Air Force Station, Tennessee.




☆ U.S. GOVERNMENT PRINTING OFFICE: 1985—679-099